Differential Rotation Profiles in Hypermassive Neutron Stars

Matthias Hanauske

Johann Wolfgang Goethe-University
Institute for Theoretical Physics
Department of Relativistic Astrophysics
Max-von-Laue-Str. 1
D-60438 Frankfurt am Main
Germany

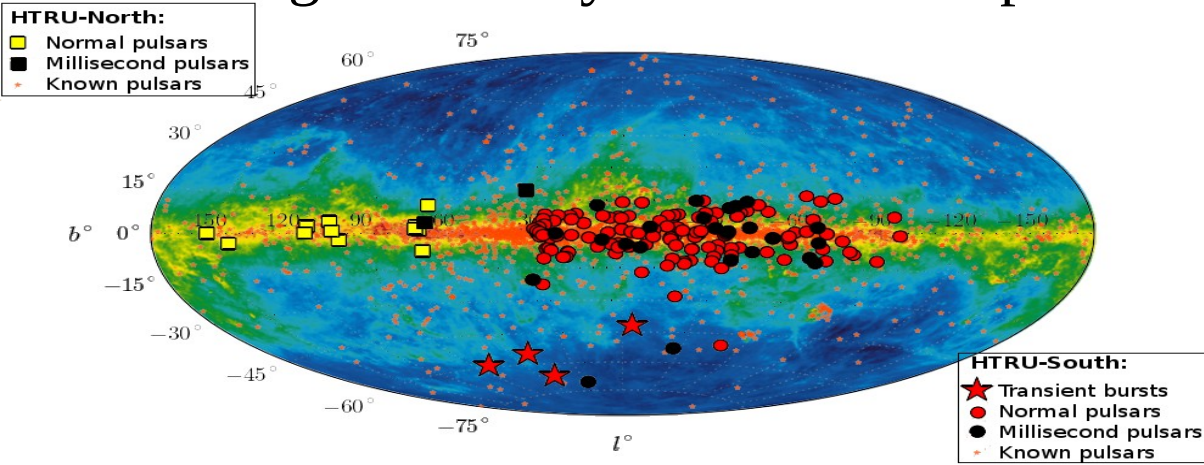**_Realistic Rotation Profiles in Hyper Massive Neutron Stars_**

Kentaro Takami, Matthias Hanauske, Luciano Rezzolla, Filippo Galeazzi, Bruno Mundim, Luke Bovard and José A. Font

1. Introduction

2. Numerical Relativity and Relativistic Hydro-dynamics of Neutron Star Mergers

3. Rotation Profiles in Hyper Massive Neutron Stars
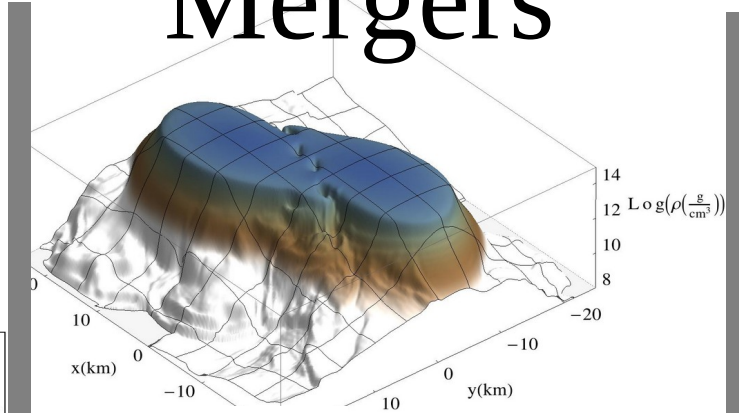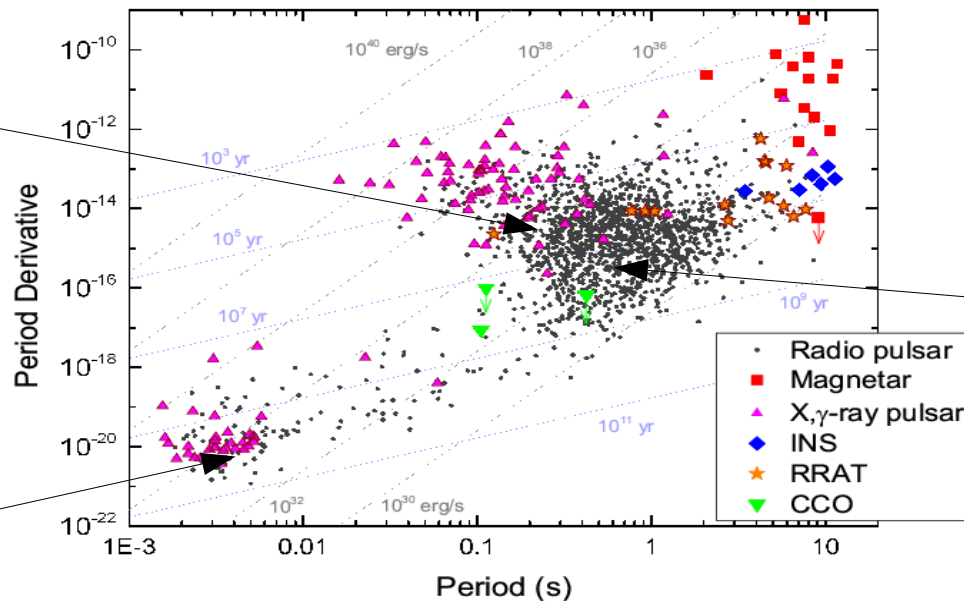
4. Summary

Pulsars

Evening Lecture by Joachim Trümpfer

Neutron Star Mergers

HTRU-North:
- Normal pulsars
- Millisecond pulsars
- Known pulsars

HTRU-South:
- ★ Transient bursts
- ● Normal pulsars
- ● Millisecond pulsars
- Known pulsars

PSR B0531+21 (33.5 ms)
Crab Pulsar

PSR B0329+54 (0.715 s)

PSR B1937+21 (1.56 ms)

Pulsars

Neutron Star Mergers

HTRU-North:
- Normal pulsars
- Millisecond pulsars
- Known pulsars

HTRU-South:
- Transient bursts
- Normal pulsars
- Millisecond pulsars
- Known pulsars

PSR B0531+21 (33.5 ms)
Crab Pulsar

PSR B0329+54 (0.715 s)
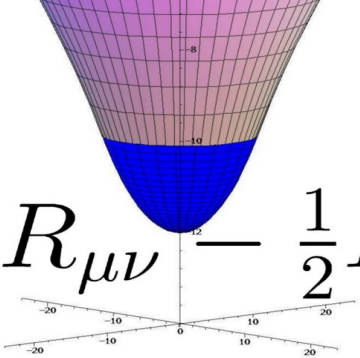
PSR B1937+21 (1.56 ms)

Realistic Rotation Profiles in Hyper Massive Neutron Stars

Kentaro Takami, Matthias Hanauske, Luciano Rezzolla, Filippo Galeazzi, Bruno Mundim, Luke Bovard and José A. Font

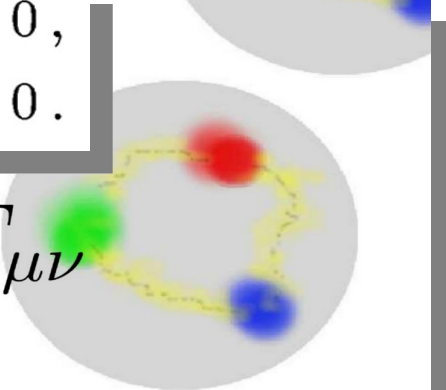# Relativistic Hydrodynamics and Numerical General Relativity

The time evolution of a merger scenario of a binary neutron star system requires the (3+1)-Split of the Einstein- and hydrodynamic equations.
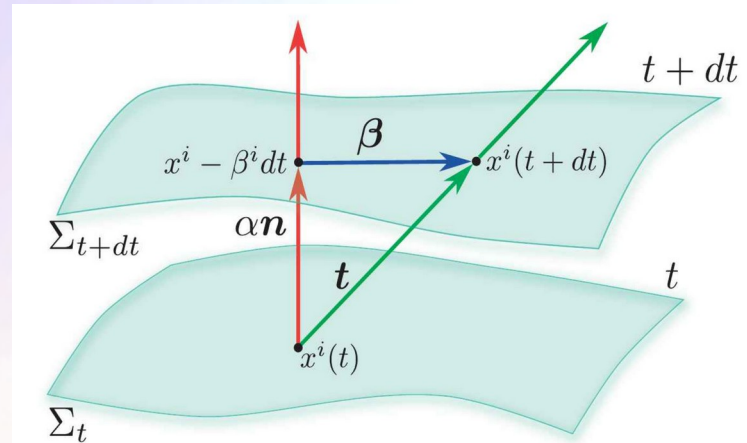
$$\nabla_\mu(\rho u^\mu) = 0\,,$$
$$\nabla_\nu T^{\mu\nu} = 0\,.$$

$$R_{\mu\nu} - \frac{1}{2}R\,g_{\mu\nu} = \frac{8\pi G}{c^4} T_{\mu\nu}$$

$$g_{\mu\nu} = \begin{pmatrix} -\alpha^2 + \beta_i\beta^i & \beta_i \\ \beta_i & \gamma_{ij} \end{pmatrix}$$

(3+1) decomposition of spacetime

$$d\tau^2 = \alpha^2(t,x^j)dt^2$$

$$x^i_{t+dt} = x^i_t - \beta^i(t,x^j)dt$$

The ADM equations

The ADM (Arnowitt, Deser, Misner) equations come from a reformulation of the Einstein equation using the (3+1) decomposition of spacetime.

$$\partial_t \gamma_{ij} = -2\alpha K_{ij} + \mathcal{L}_{\boldsymbol{\beta}}\gamma_{ij}$$
$$= -2\alpha K_{ij} + D_i\beta_j + D_j\beta_i$$

$$\partial_t K_{ij} = -D_iD_j\alpha + \beta^k\partial_k K_{ij} + K_{ik}\partial_j\beta^k + K_{kj}\partial_i\beta^k$$
$$+ \alpha\left({}^{(3)}R_{ij} + KK_{ij} - 2K_{ik}K^k_{\ j}\right) + 4\pi\alpha\left[\gamma_{ij}\left(S - E\right) - 2S_{ij}\right]$$

Time evolving part of ADM

$$D_j(K^{ij} - \gamma^{ij}K) = 8\pi S^i$$

$${}^{(3)}R + K^2 - K_{ij}K^{ij} = 16\pi E$$

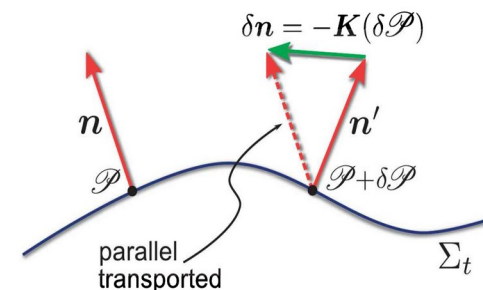Constraints on each hypersurface

Three dimensional covariant derivative

$$D_\nu := \gamma^\mu_{\ \nu}\nabla_\mu = (\delta^\mu_\nu + n_\nu n^\mu)\nabla_\mu$$

Spatial and normal projections of the energy-momentum tensor:

$$S_{\mu\nu} := \gamma^\alpha_{\ \mu}\,\gamma^\beta_{\ \nu}\,T_{\alpha\beta}\,,$$
$$S_\mu := -\gamma^\alpha_{\ \mu}\,n^\beta T_{\alpha\beta}\,,$$
$$S := S^\mu_{\ \mu}\,,$$
$$E := n^\alpha\,n^\beta T_{\alpha\beta}\,,$$
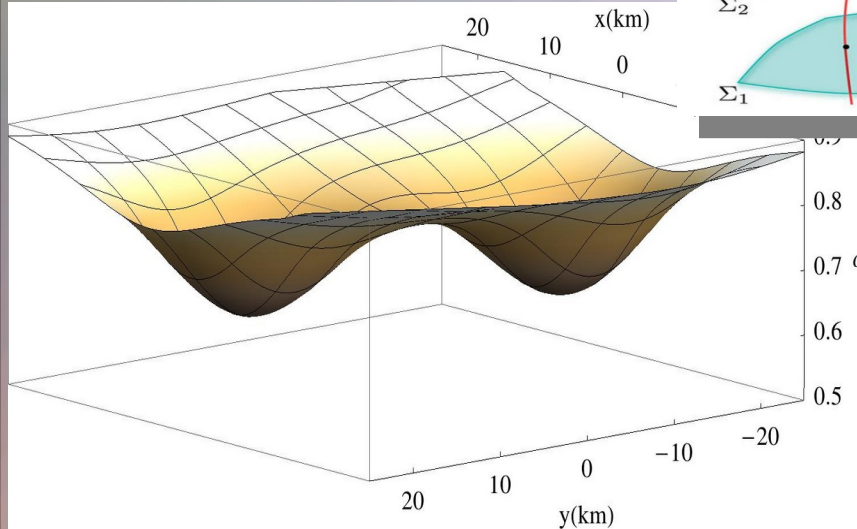
Extrinsic Curvature:
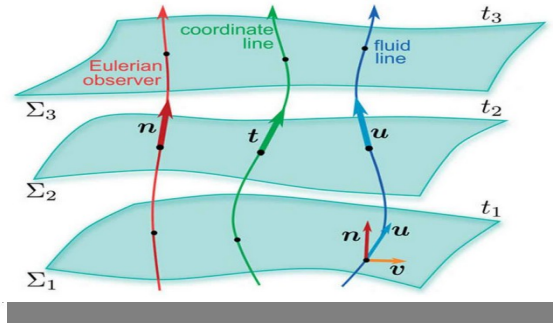
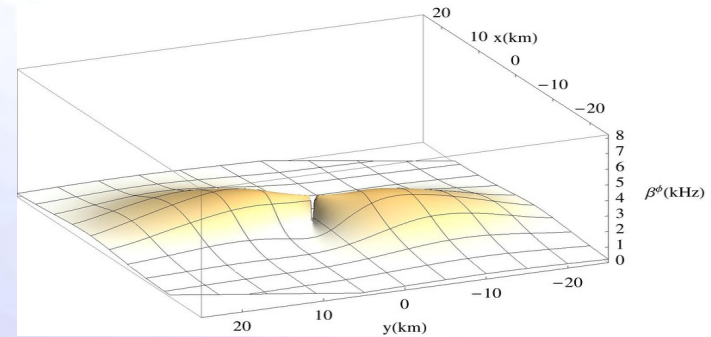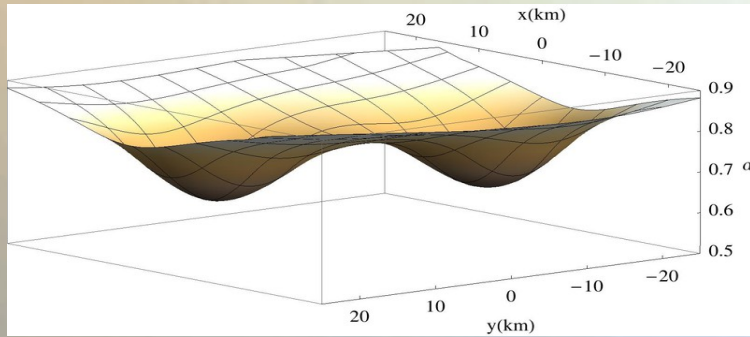$$K_{\mu\nu} := -\gamma^\lambda_{\ \mu}\nabla_\lambda n_\nu$$
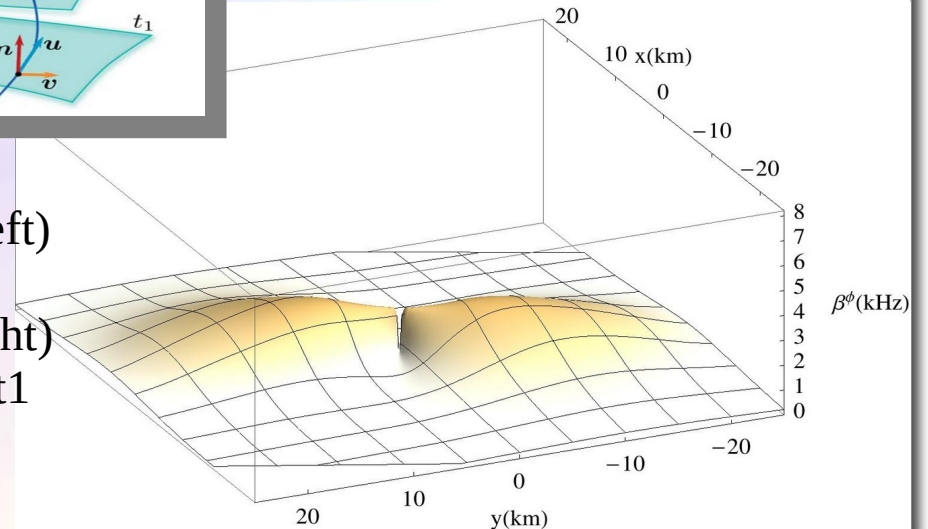
Three dimensional Riemann tensor

$${}^{(3)}R^\mu_{\ \nu\kappa\sigma} = \partial_\kappa\,{}^{(3)}\Gamma^\mu_{\nu\sigma} - \partial_\sigma\,{}^{(3)}\Gamma^\mu_{\nu\kappa} + {}^{(3)}\Gamma^\mu_{\lambda\kappa}\,{}^{(3)}\Gamma^\lambda_{\nu\sigma} - {}^{(3)}\Gamma^\mu_{\lambda\sigma}\,{}^{(3)}\Gamma^\lambda_{\nu\kappa}$$

$${}^{(3)}\Gamma^\alpha_{\beta\gamma} = \frac{1}{2}\gamma^{\alpha\delta}\left(\partial_\beta\gamma_{\gamma\delta} + \partial_\gamma\gamma_{\delta\beta} - \partial_\delta\gamma_{\beta\gamma}\right)$$

$\delta n = -K(\delta\mathscr{P})$
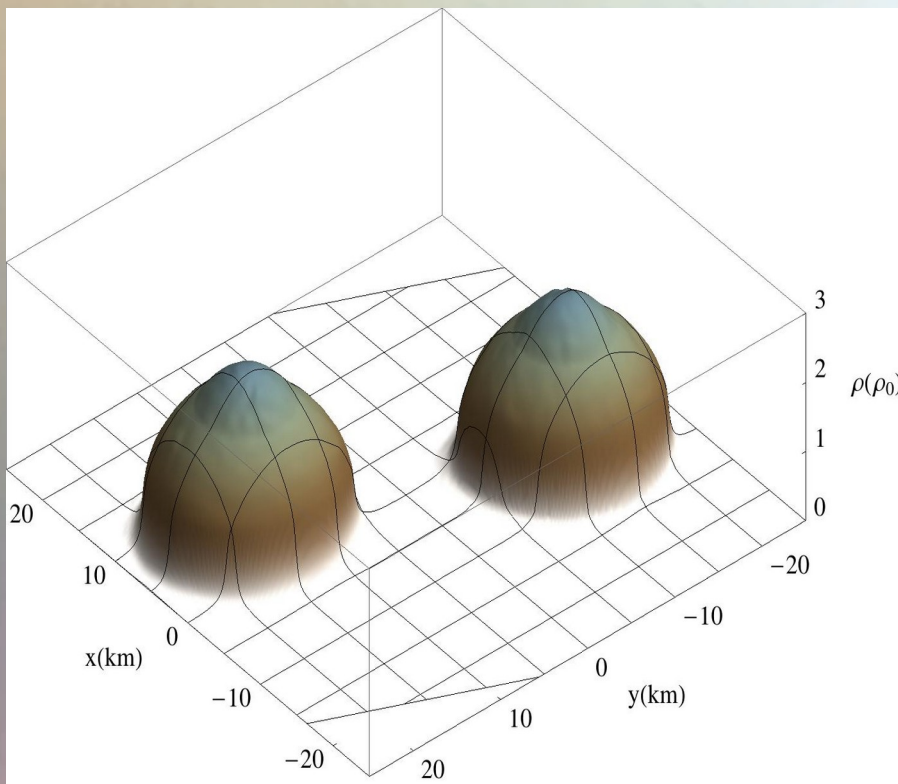
n n'

$\mathscr{P}$ $\mathscr{P}+\delta\mathscr{P}$

parallel transported Σ_t

Evolution of Lapse and Shift

Lapse (left) and Shift (right) at time t1

Relativistic Hydrodynamics

Simulations where done by
Kentaro Takami

BSSNOK conformal traceless formulation of the ADM equations. 3+1 Valencia formulation and high resolution shock capturing methods for the hydodynamic evolution. Simulations have been performed in full general relativity using the WHISKY code for the general-relativistic hydrodynamic equations and 5 EoS:
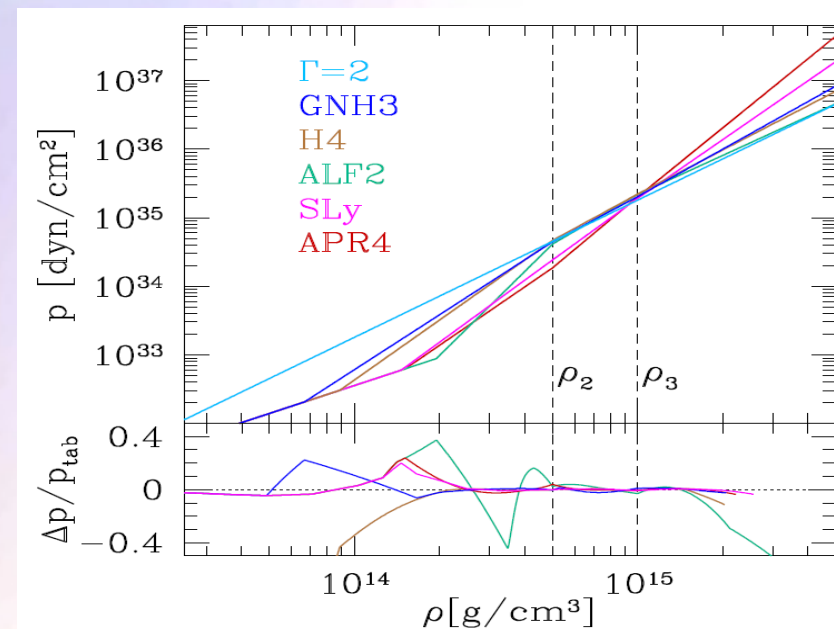
Relativistic Hydrodynamics

BSSNOK conformal traceless formulation of the ADM equations. 3+1 Valencia formulation and high resolution shock capturing methods for the hydodynamic evolution. Simulations have been performed in full general relativity using the WHISKY code for the general-relativistic hydrodynamic equations and 5 EoS:
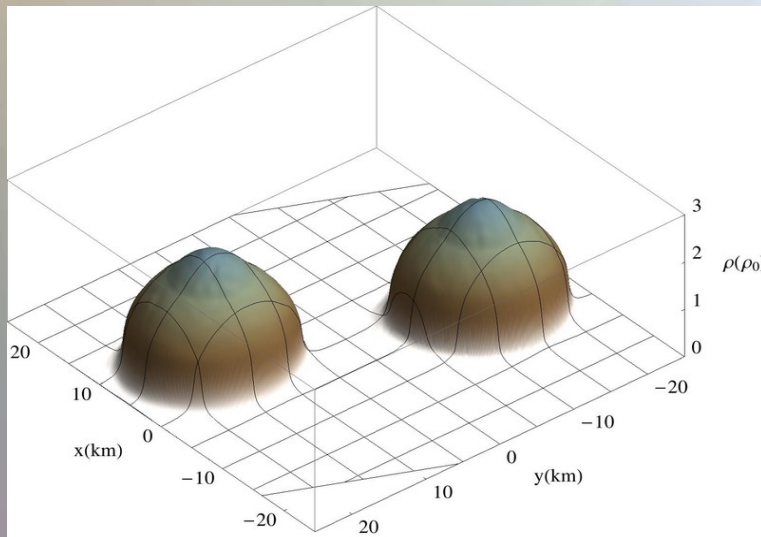

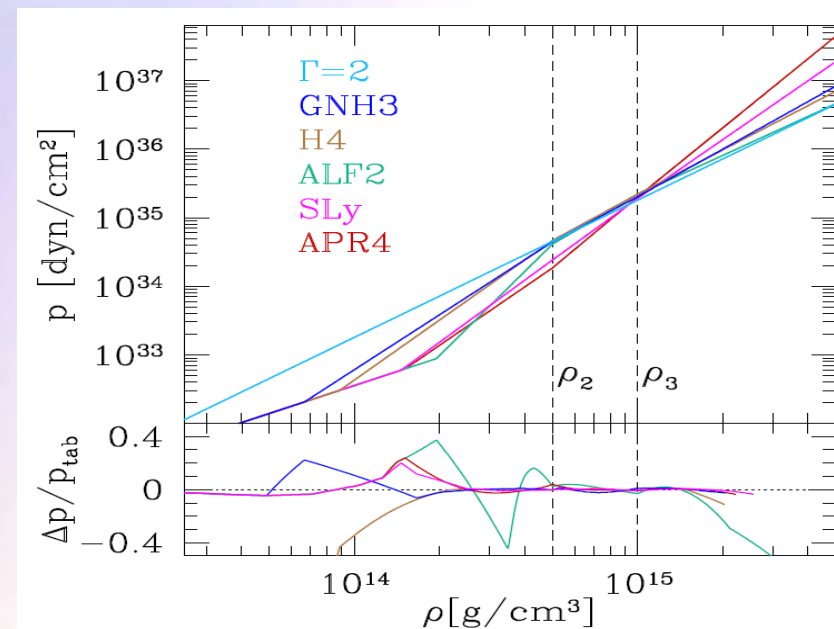Simulations where done by Kentaro Takami

Relativistic Hydrodynamics

BSSNOK conformal traceless formulation of the ADM equations. 3+1 Valencia formulation and high resolution shock capturing methods for the hydodynamic evolution. Simulations have been performed in full general relativity using the WHISKY code for the general-relativistic hydrodynamic equations and 5 EoS:
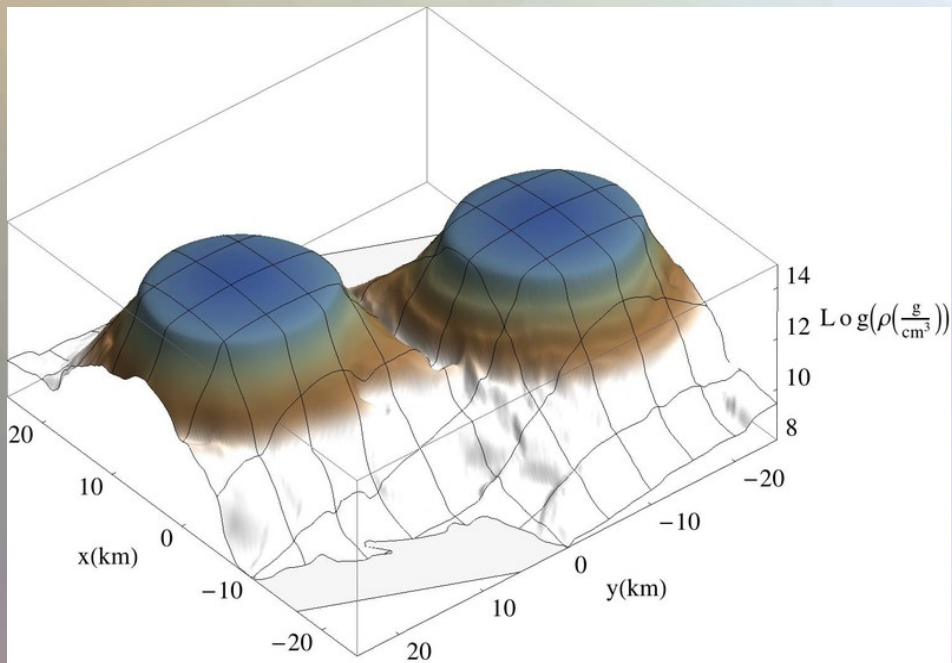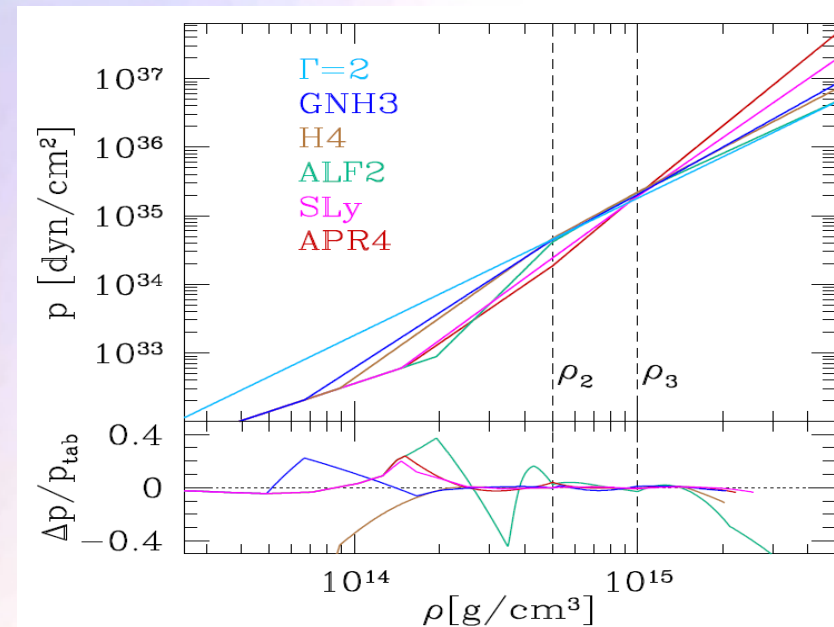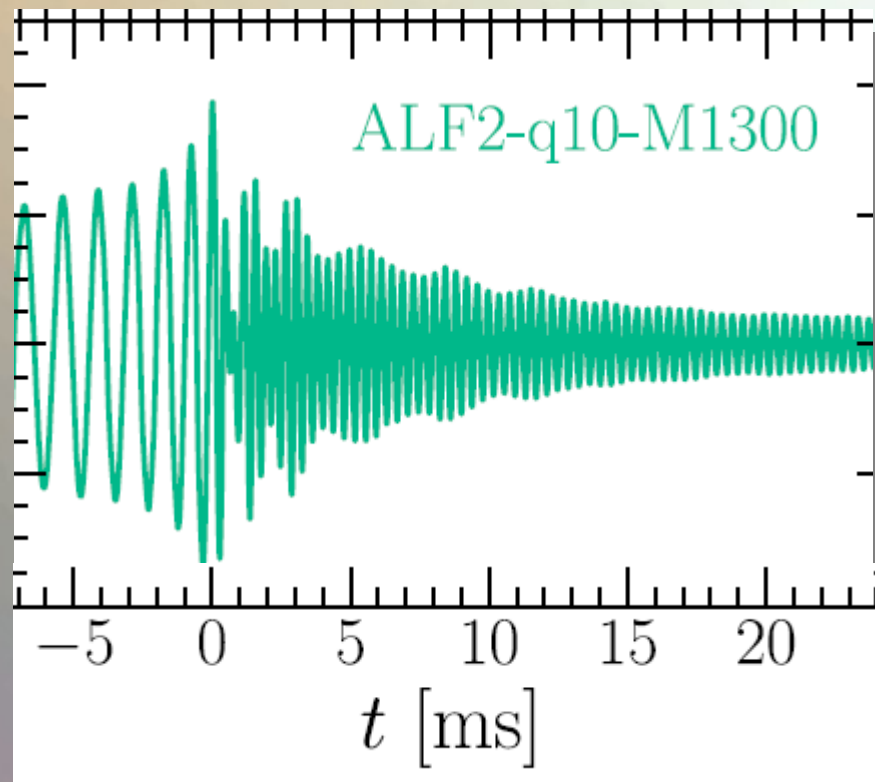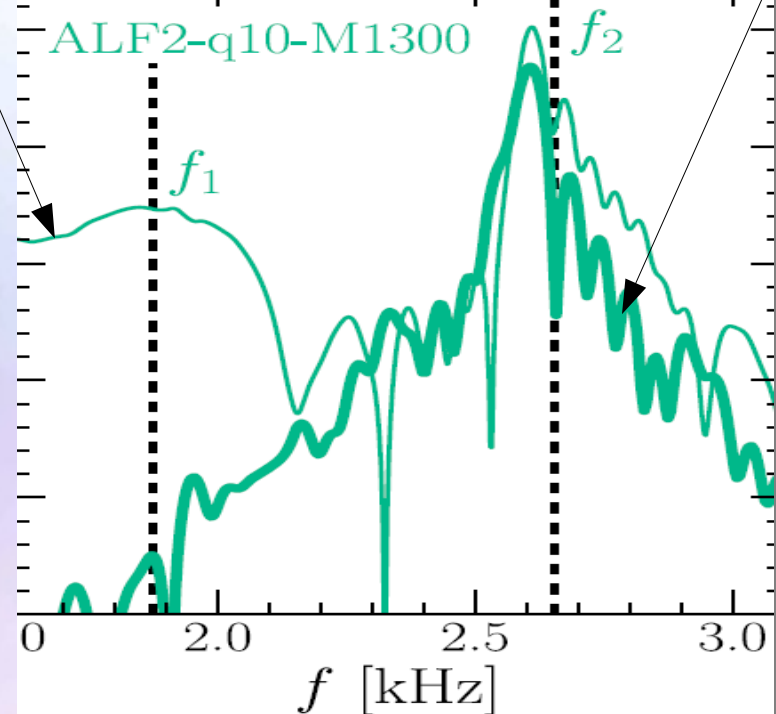

Simulations where done by
Kentaro Takami

Gravitational Waves

Talk by Luciano Rezzolla

Full spectral profile (thin curve)

Spectral profile (t >3 ms) (thick curve)

The Power Spectral Density (PSD) of the emitted gravitational waves show for all of the EoS a similar spectral property with two characteristic frequency peaks (f_1 and f_2). The origin of f_1 comes from t<3 ms.

***Realistic Rotation Profiles in Hyper Massive Neutron Stars***

Kentaro Takami, Matthias Hanauske, Luciano Rezzolla, Filippo Galeazzi, Bruno Mundim, Luke Bovard and José A. Font

1. Introduction

2. Numerical Relativity and Relativistic Hydro-dynamics of Neutron Star Mergers

3. **Rotation Profiles in Hyper Massive Neutron Stars (HMNS)**

4. Summary

The Angular Velocity in the (3+1)-Split

$$\Omega(x, y, z, t) = \Omega = \quad \frac{d\phi}{dt} = \frac{dx^\phi}{dt} = \qquad \text{with:} \quad x^\mu = (t, r, \phi, \theta)$$

$$= \frac{dx^\phi}{dt} = \frac{\frac{dx^\phi}{d\tau}}{\frac{dt}{d\tau}} = \frac{u^\phi}{u^t} \; (1) \quad \text{with:} \quad u^\mu = \frac{dx^\mu}{d\tau}$$
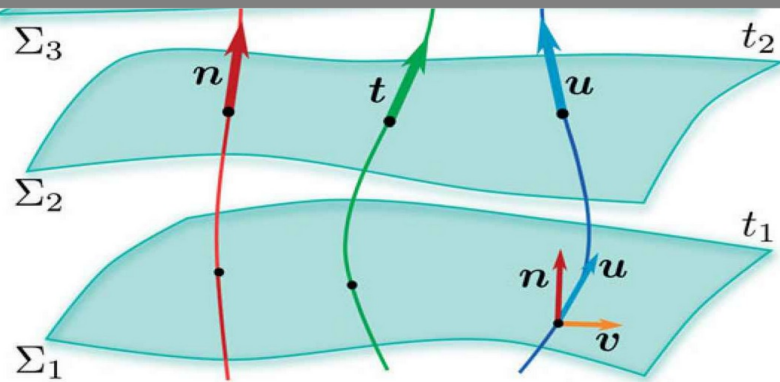
The angular velocity in the (3+1)-Split is a combination of the lapse function, the phi-component of the shift vector and the 3-velocity **v** of the fluid (spatial projection of the 4-velocity **u**)
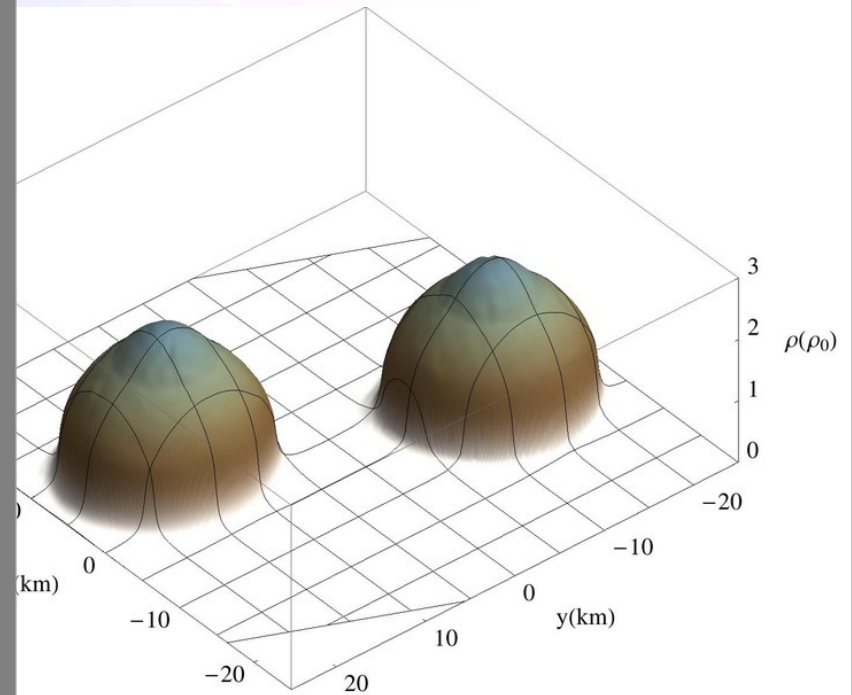
$$v^i = \frac{\gamma^i_\mu u^\mu}{-n_\mu u^\mu} = \frac{1}{\alpha}\left(\frac{u^i}{u^t} - \beta^i\right) \qquad \text{with:} \quad i = 1, 2, 3 \text{ and } \mu = 0, 1, 2, 3$$

$$\Leftrightarrow \quad \frac{u^i}{u^t} = \alpha v^i - \beta^i \qquad \text{Insert in (1)} \Rightarrow \qquad \Omega = \frac{d\phi}{dt} = \frac{u^\phi}{u^t} = \alpha v^\phi - \beta^\phi$$
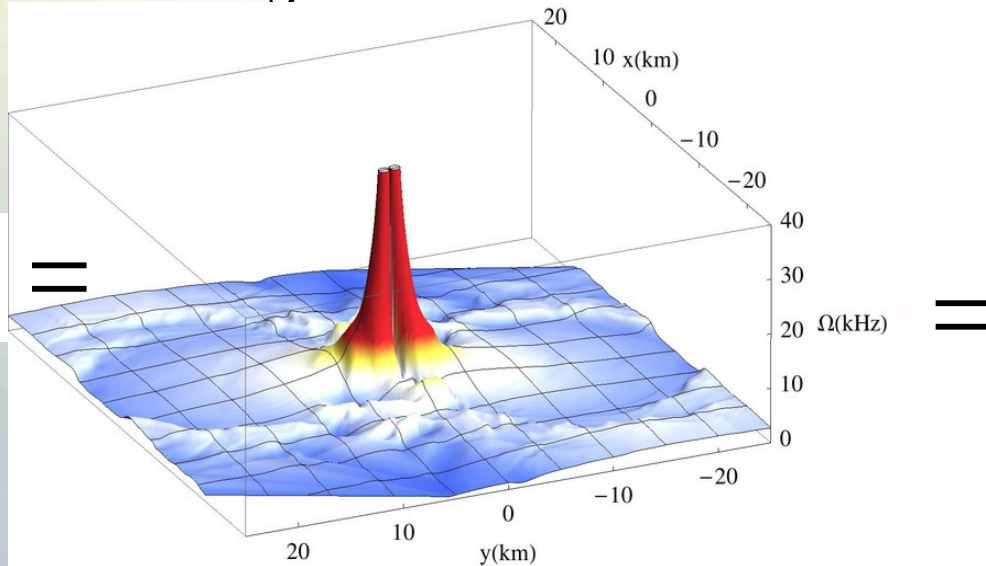
EoS: ALF2, M=1.35
Inspiral and Merger Phase
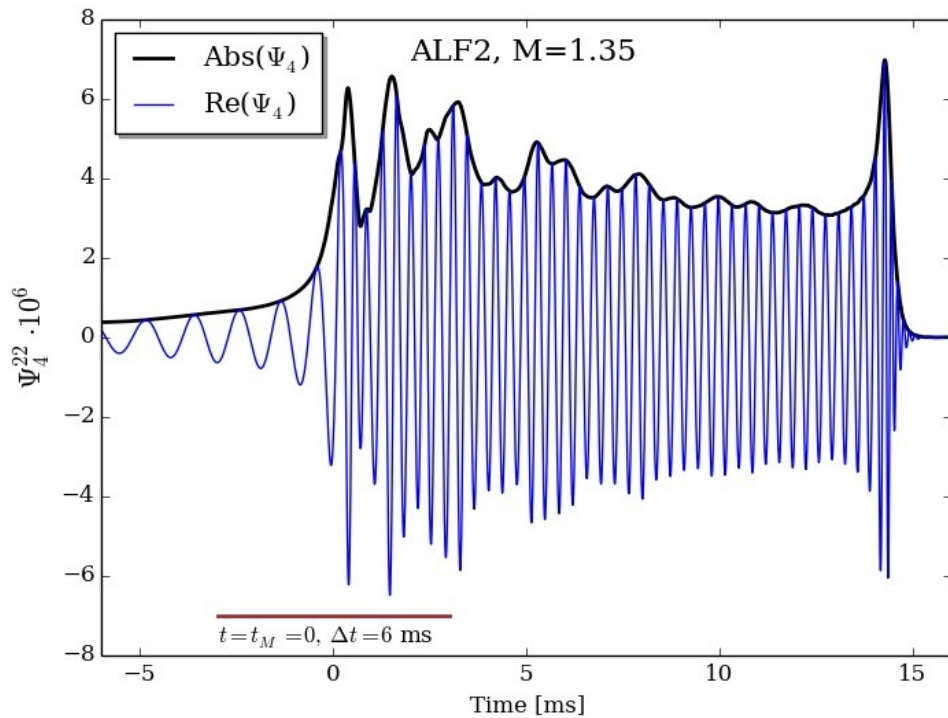
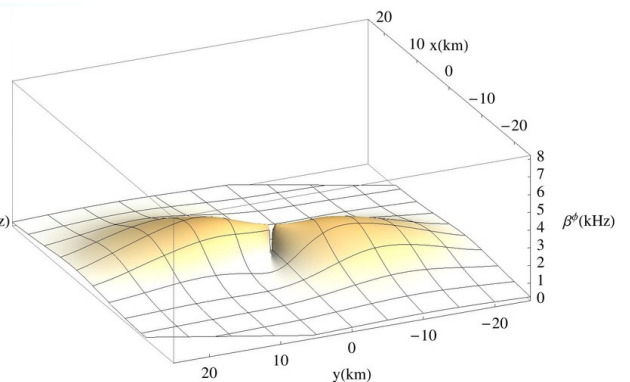# Angular Velocity Rotation Profile

Inspiral and Merger

$$\Omega(x, y, z, t)|_{z=0} = \quad = $$

$$\alpha(x, y, t) \quad \cdot \quad v^{\phi}(x, y, t) \quad - \quad \beta^{\phi}(x, y, t)$$
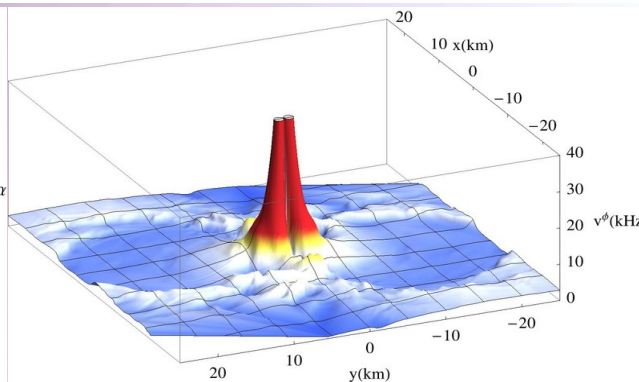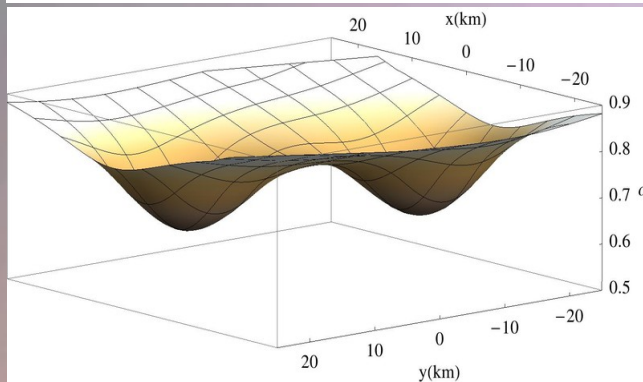
EoS: ALF2, M=1.35
Post Merger Phase
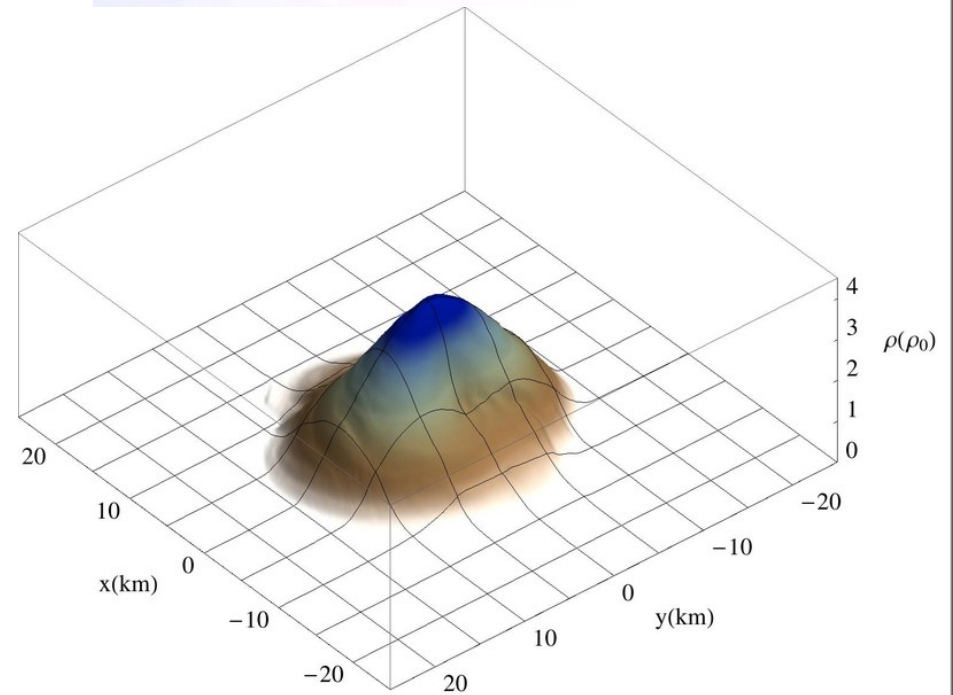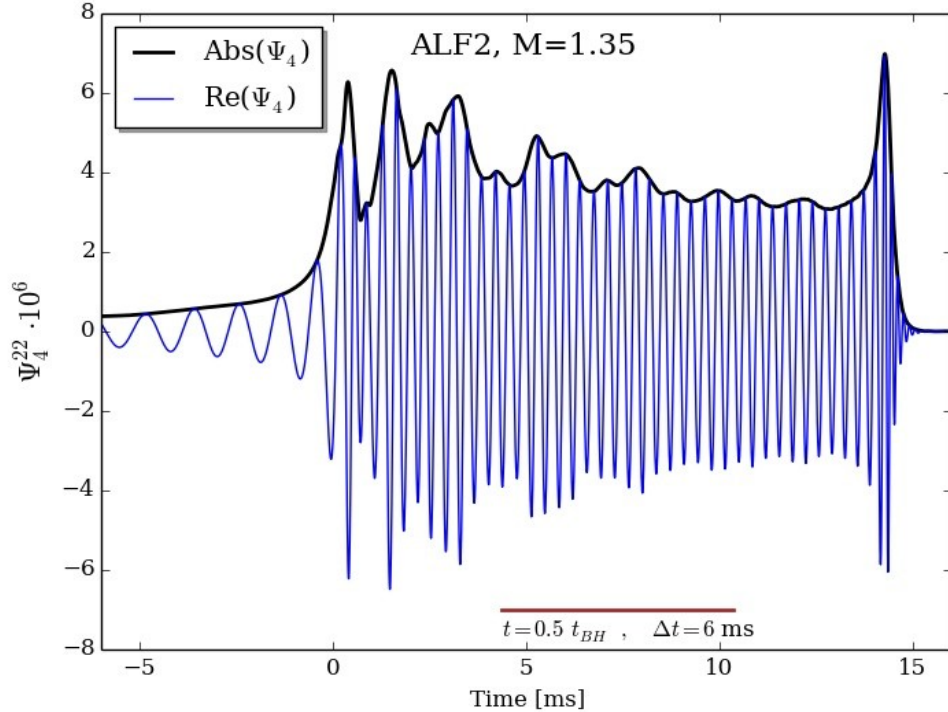
Angular Momentum Rotation Profile
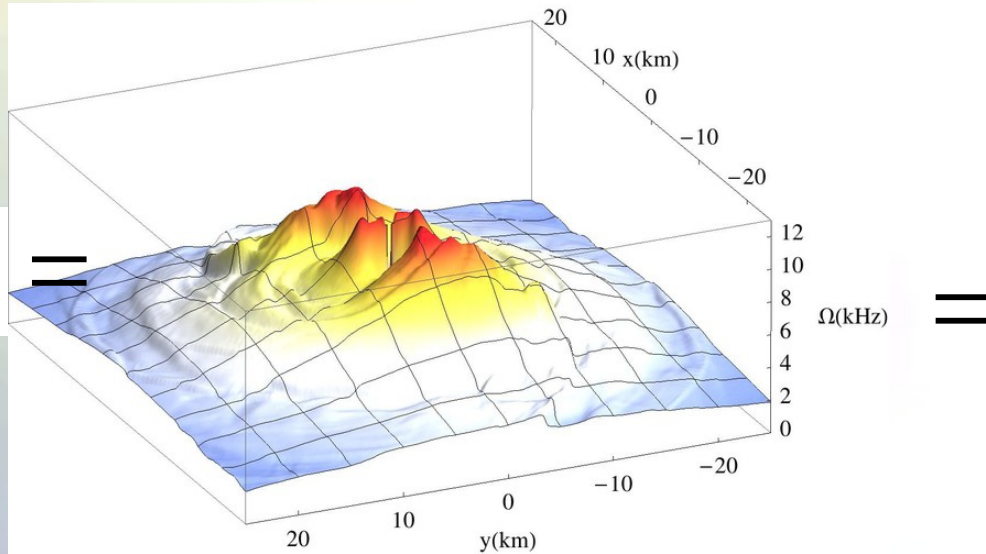
Post Merger
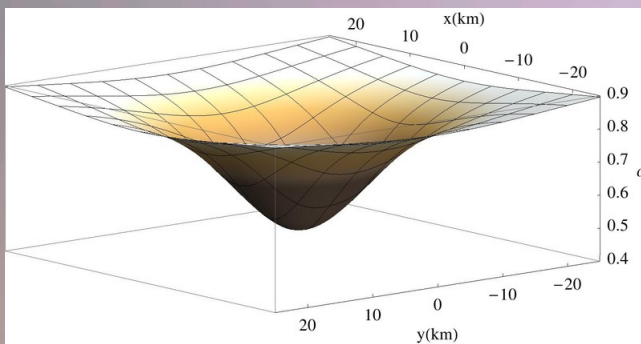
$$\Omega(x, y, z, t)\big|_{z=0} =$$

$$\alpha(x, y, t) \quad \cdot \quad v^\phi(x, y, t) \quad - \quad \beta^\phi(x, y, t)$$

EoS: ALF2, M=1.35
Black Hole Formation Phase
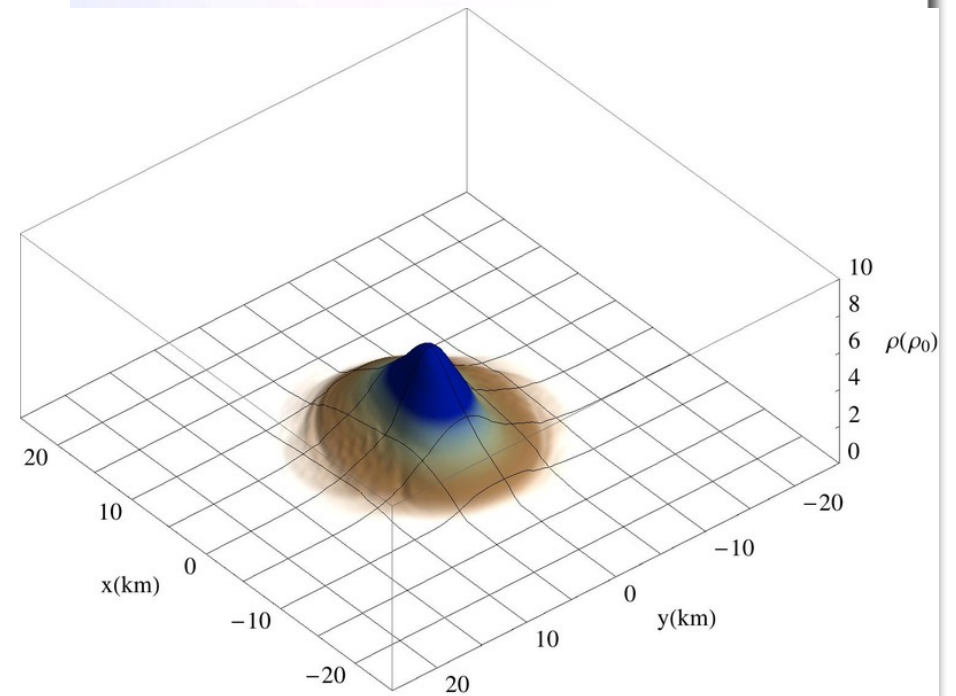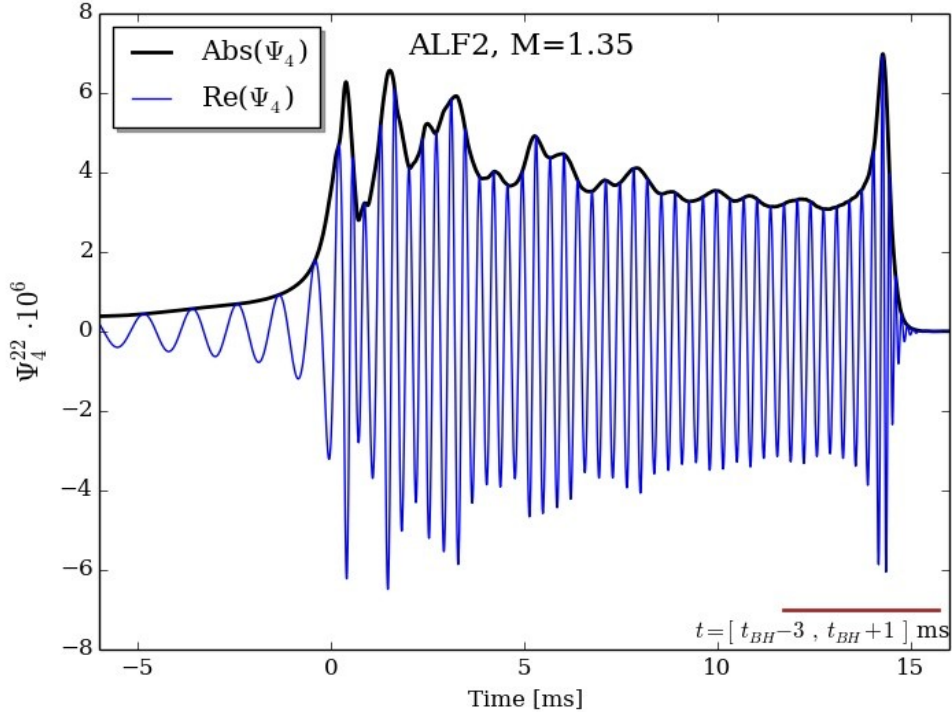
Angular Momentum Rotation Profile

BH Formation

$$\Omega(x, y, z, t)|_{z=0} = $$

$$= $$
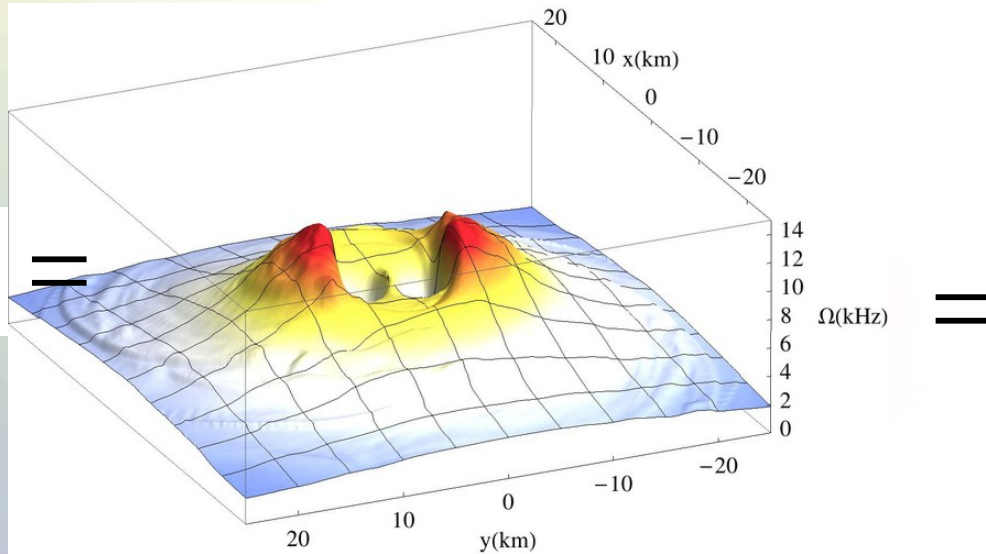
$$\alpha(x, y, t) \quad \cdot \quad v^\phi(x, y, t) \quad - \quad \beta^\phi(x, y, t)$$
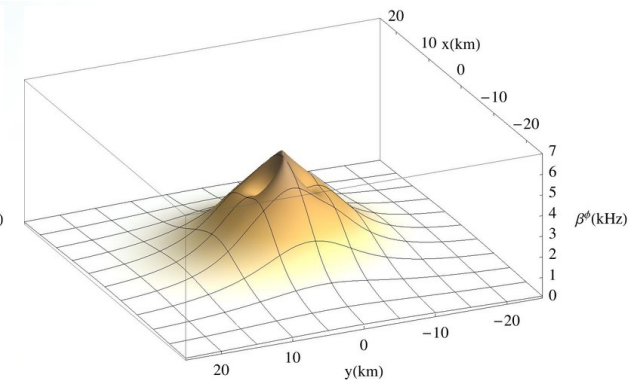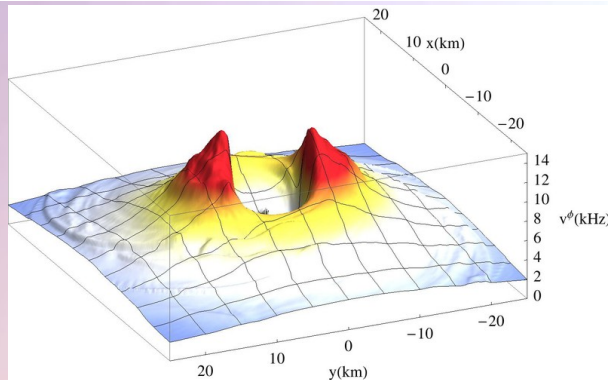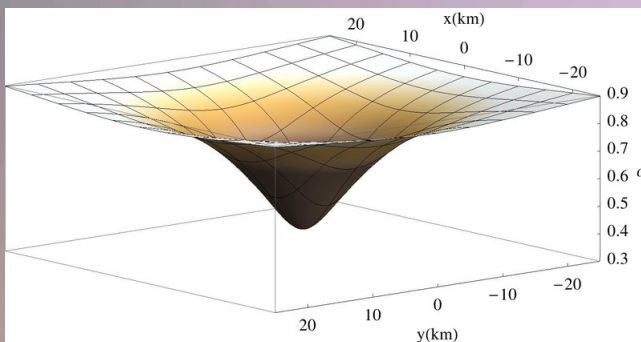
EoS: ALF2, M=1.25
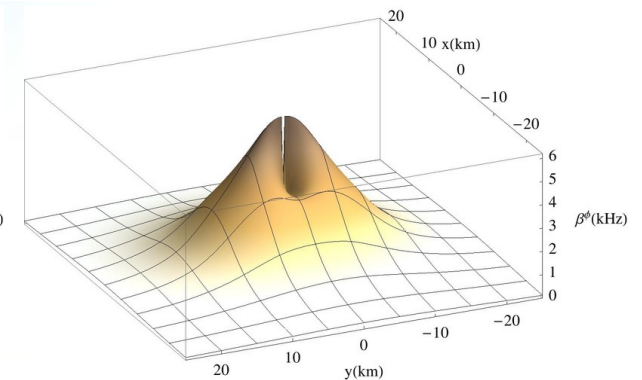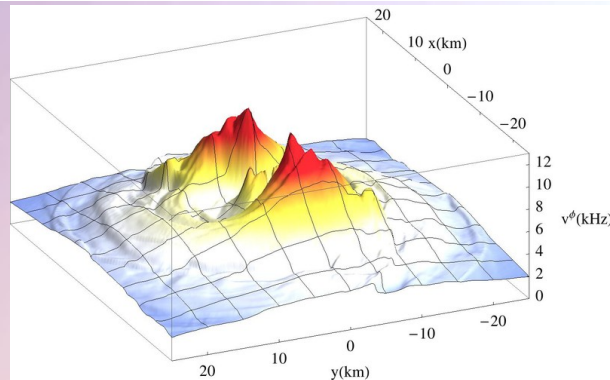## Post Merger Phase
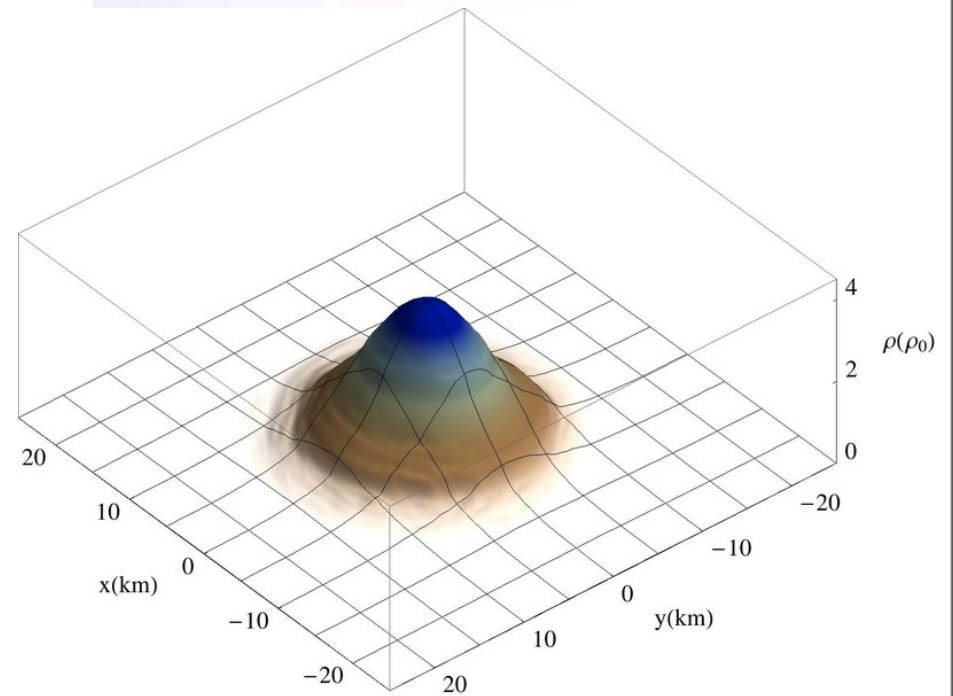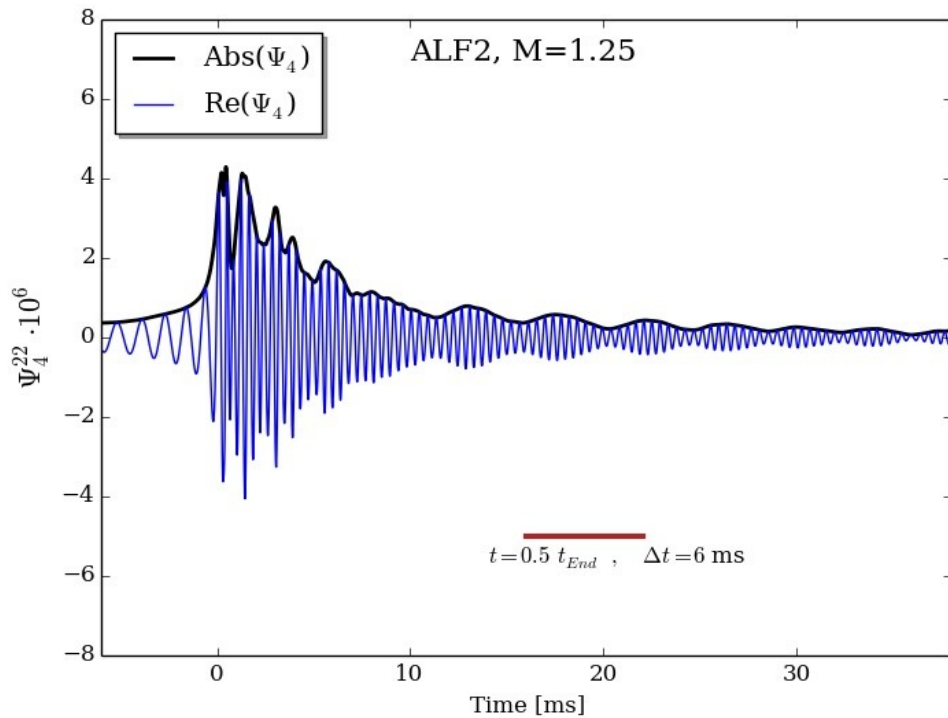
Angular Momentum Rotation Profile

Post Merger

$$\left.\Omega(x, y, z, t)\right|_{z=0} =$$

$= \qquad =$
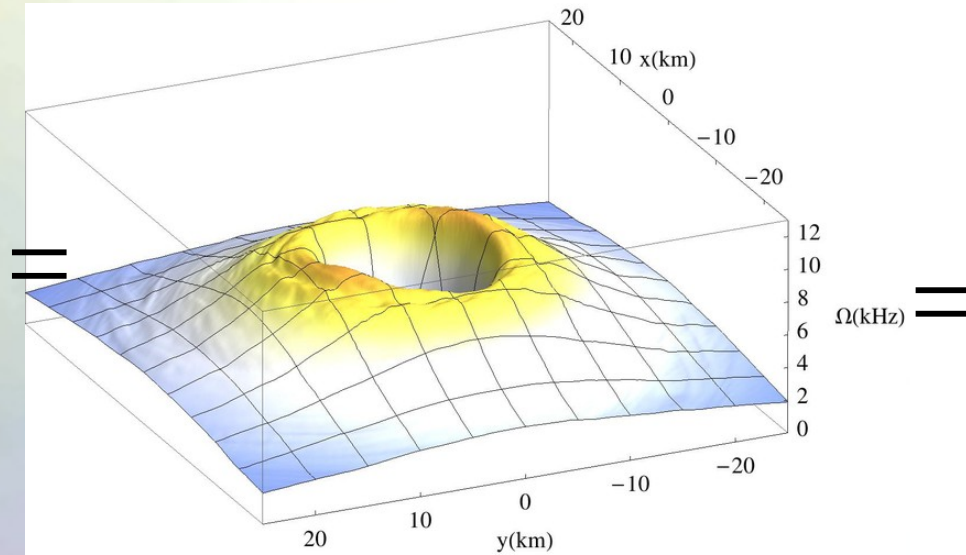
$$\alpha(x, y, t) \qquad \cdot \qquad v^{\phi}(x, y, t) \qquad - \qquad \beta^{\phi}(x, y, t)$$
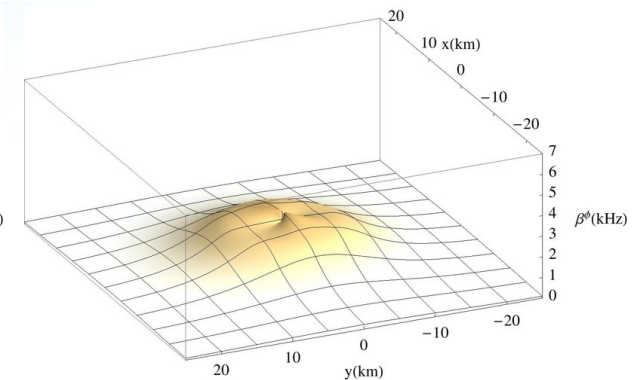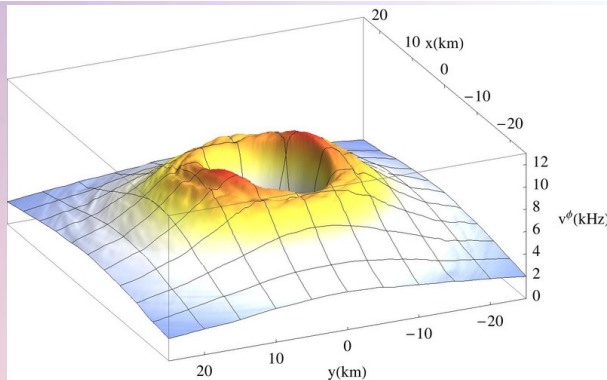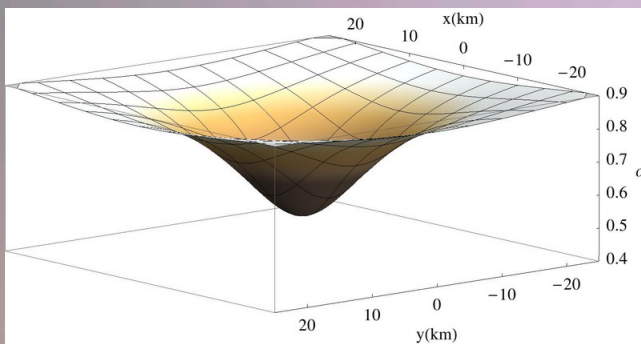
Dependence on the EoS
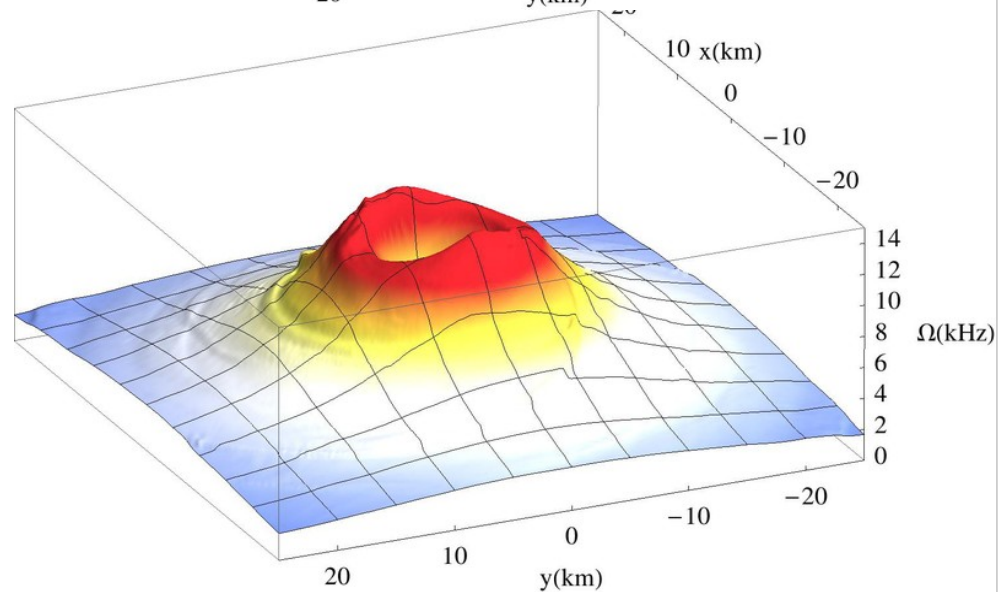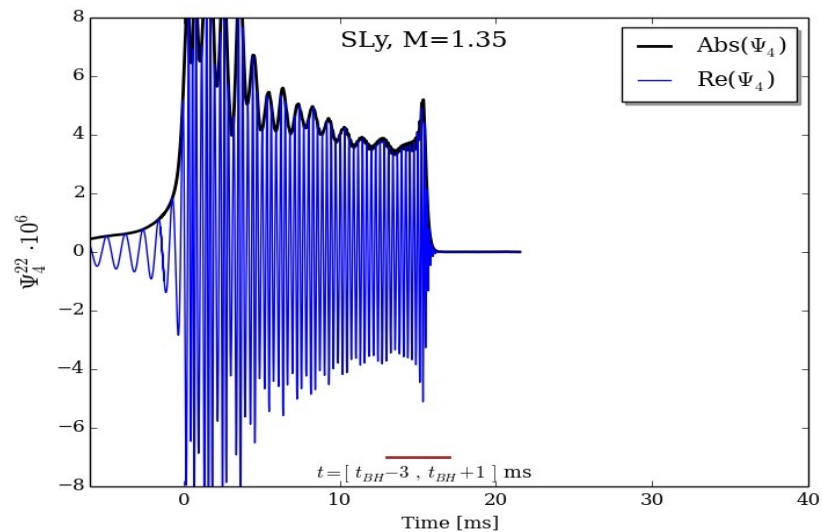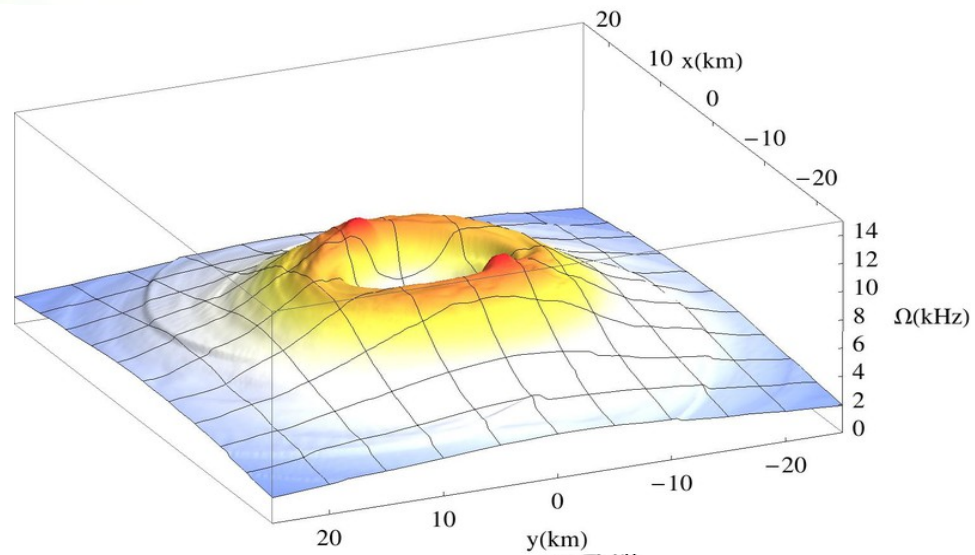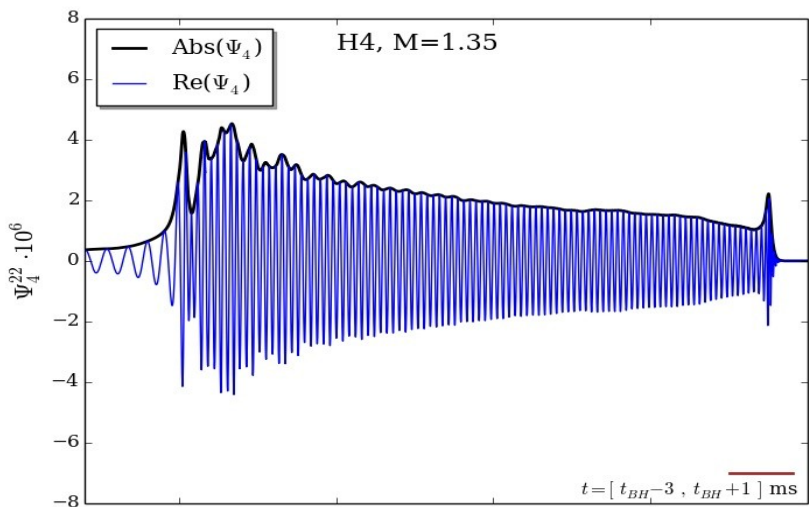
Rotation Profile H4, M=1.35

Post Merger

$$\Omega(x, y, z, t)|_{z=0} =$$
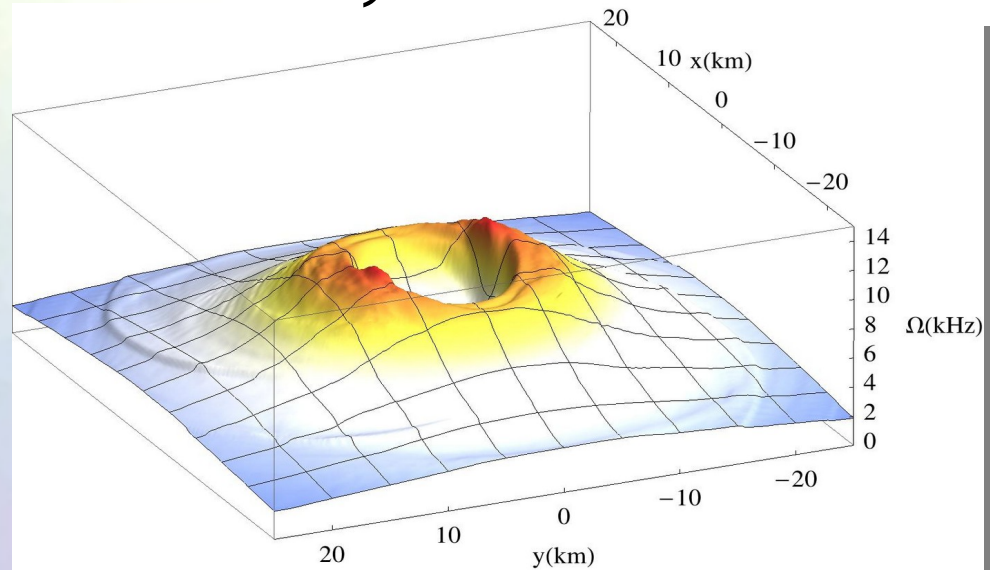
$$\Omega(r, \phi, z, t)|_{z=0} =$$
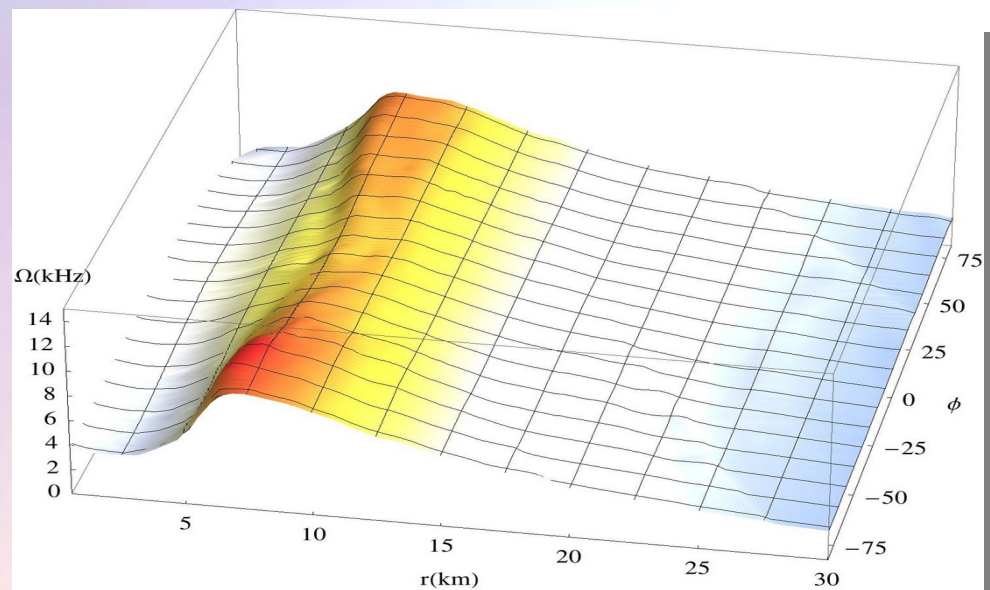
Realistic Rotation Profiles
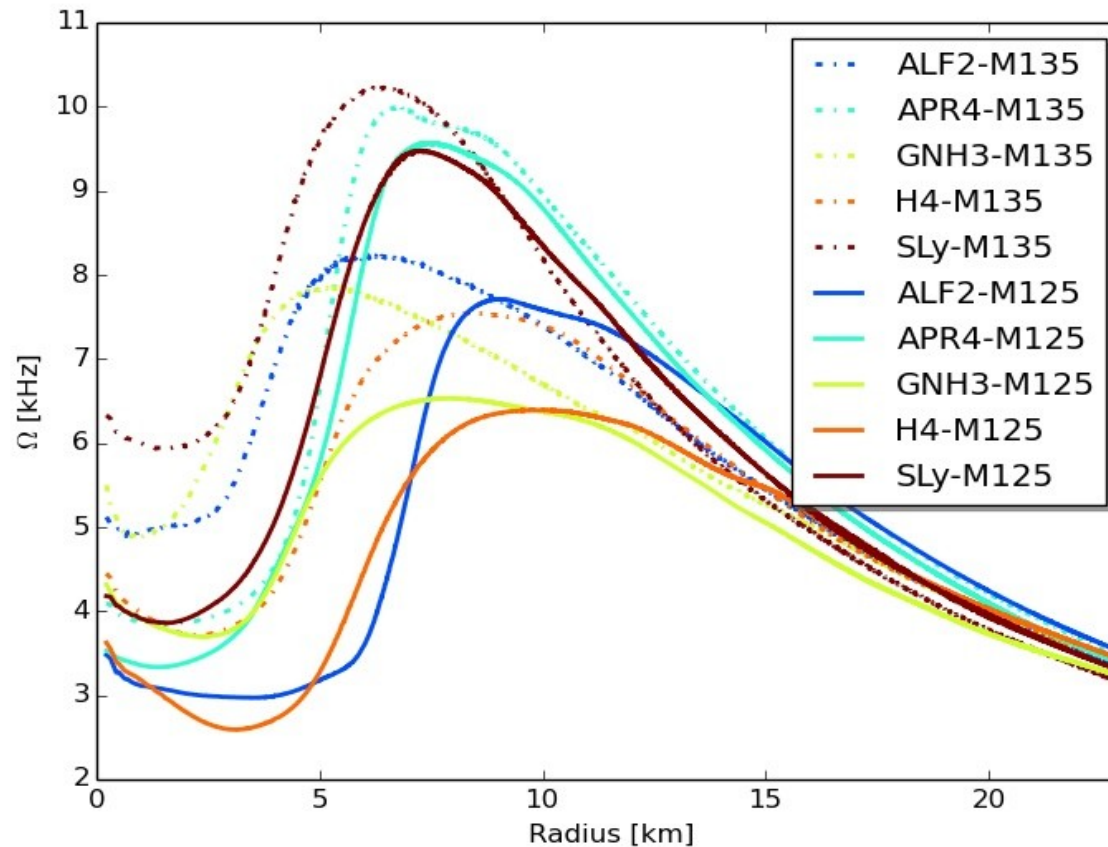
Summary

1. The differential rotation profiles of the hyper massive neutron stars (HMNS) in the merger, post-merger and black hole formation phase have been analyzed.

2. The simulations have been performed in full general relativity using the WHISKY code for the general relativistic hydrodynamic equations.

3. The HMNS rotation profiles show a structural uniqueness in respect to a variation of the EoS and initial neutron star mass.

End

- ….Additional, backup-slides follow

Rotation Profile ALF2, M=1.35

Post Merger

$$\Omega(x, y, z, t)|_{z=0} =$$
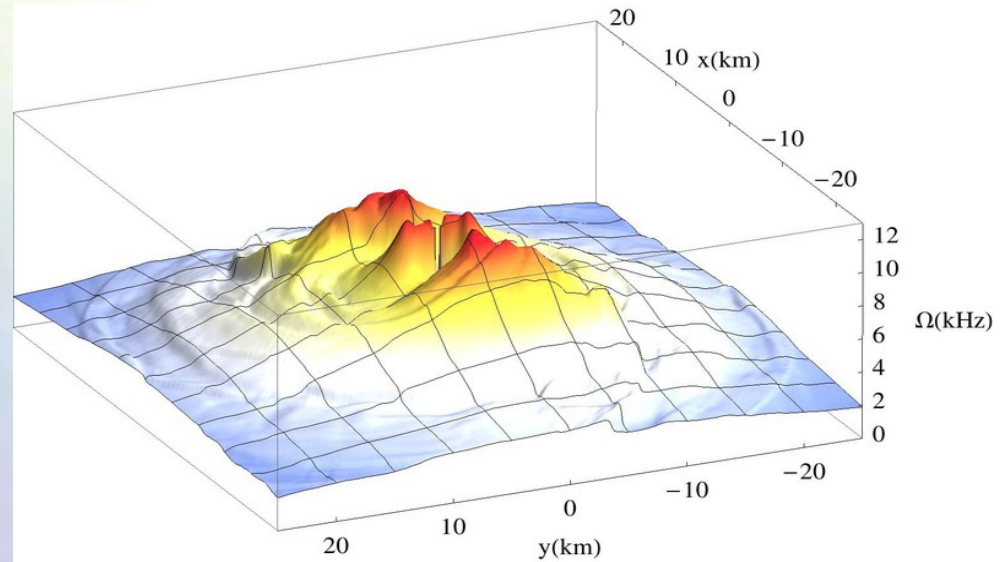
$$\Omega(r, \phi, z, t)|_{z=0} =$$
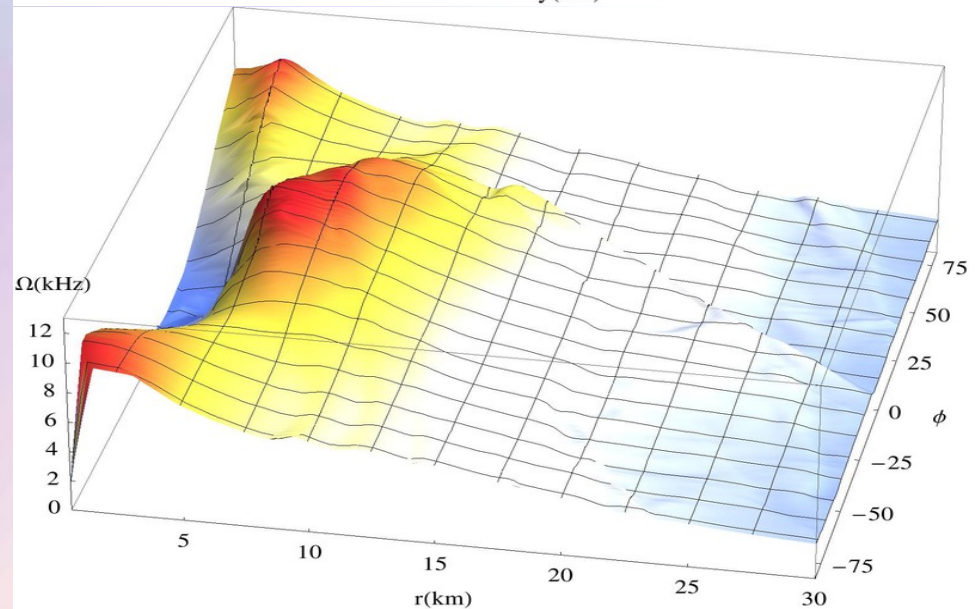
Gauge Conditions

On each spatial hypersurface, four additional degrees of freedom need to be specified: A *slicing condition* for the lapse function and a *spatial shift condition* for the shift vector need to be formulated to close the system. In an optimal gauge condition, singularities should be avoided and numerical calculations should be less time consuming.

Bona-Massó family of slicing conditions:

$$\partial_t \alpha - \beta^k \partial_k \alpha = -f(\alpha)\, \alpha^2 (K - K_0)$$

"1+log" slicing condition: $f = 2/\alpha$

where $f(\alpha) > 0$ and $K_0 := K(t = 0)$

"Gamma-Driver" shift condition:

$$\partial_t \beta^i - \beta^j \partial_j \beta^i = \frac{3}{4} B^i,$$

$$\partial_t B^i - \beta^j \partial_j B^i = \partial_t \tilde{\Gamma}^i - \beta^j \partial_j \tilde{\Gamma}^i - \eta B^i$$

General Relativity and Quantum Cromodynamics

	ART	Yang-Mills-Theories
	$D_\beta v^\alpha = \partial_\beta v^\alpha + \Gamma^\alpha_{\sigma\beta} v^\sigma$	$D_{\beta a}{}^b = \partial_\beta 1_a{}^b + ig A_{\beta a}{}^b$
	$R^\delta{}_{\mu\alpha\beta} v^\mu = [D_\alpha, D_\beta] v^\delta$	$F_{\alpha\beta a}{}^b = \frac{1}{ig}\left[D_{\alpha a}{}^c, D_{\beta c}{}^b\right]$
	$R^\delta{}_{\mu\alpha\beta} = \Gamma^\delta_{\mu\alpha|\beta} - \Gamma^\delta_{\mu\beta|\alpha}$	$= A_{\beta a}{}^b{}_{|\alpha} - A_{\alpha a}{}^b{}_{|\beta}$
	$+\Gamma^\delta_{\nu\beta}\Gamma^\nu_{\mu\alpha} + \Gamma^\delta_{\nu\alpha}\Gamma^\nu_{\mu\beta}$	$+\frac{1}{ig}\left[A_{\alpha a}{}^c, A_{\beta c}{}^b\right]$
	$\mathcal{L}_G = R + \underbrace{(c_1 R_{\mu\nu}R^{\mu\nu} + ...)}_{\equiv 0 \text{ for } ART}$	$\mathcal{L}_{YM} = \frac{1}{4}F_{\mu\nu a}{}^b F^{\mu\nu}{}_a{}^b$

QuantumCromoDynamic:

$(SU(3)_{(c)}$- Color Yang-Mills-Gauge Theory)

$$D_{\beta A}{}^B = \partial_\beta 1_A{}^B + ig G_{\beta A}{}^B$$

$_A,{}^B$ =red, green, blue
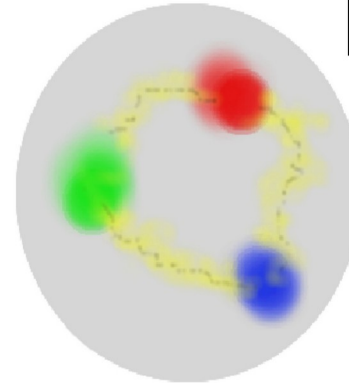
$$\psi_A^f = \begin{pmatrix} \psi_r^f \\ \psi_g^f \\ \psi_b^f \end{pmatrix}$$

Confinement
chiral symmetry, ...
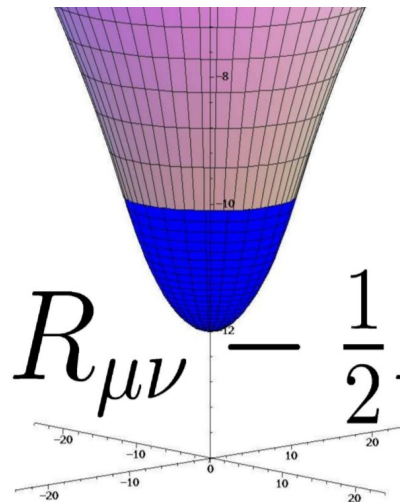
$$R_{\mu\nu} - \frac{1}{2}R\,g_{\mu\nu} = \frac{8\pi G}{c^4} T_{\mu\nu}$$
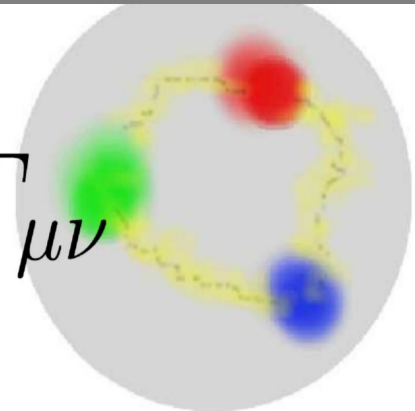
The QCD – Phase Transition and the Interior of a Hybrid Star
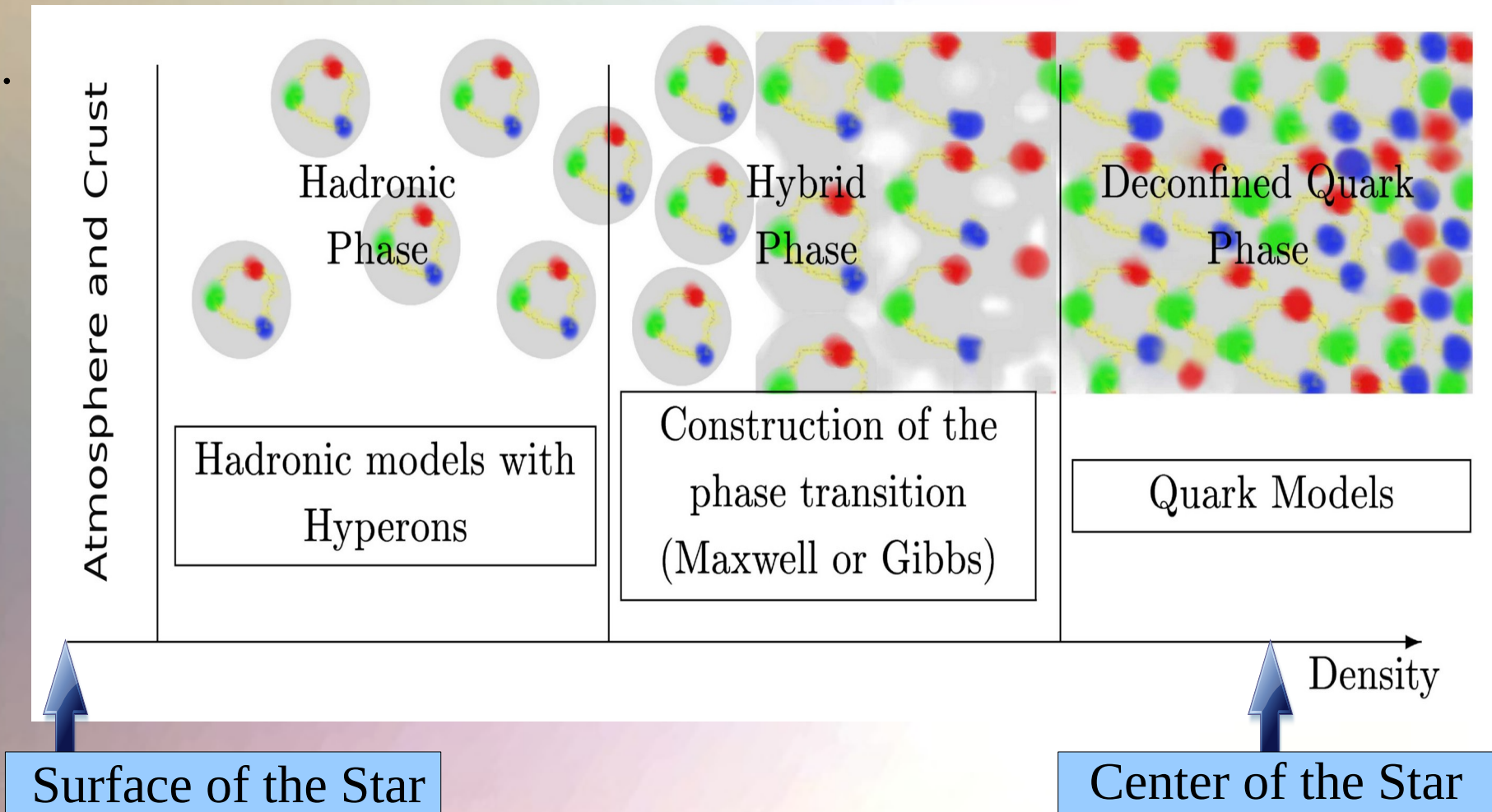
The Compact Star Zoo

Neutron stars with and without hyperons, quark stars and strange quark stars, hybrid stars with color superconducting quark matter, hybrid stars with Bose-Einstein condensates of antikaons, ...
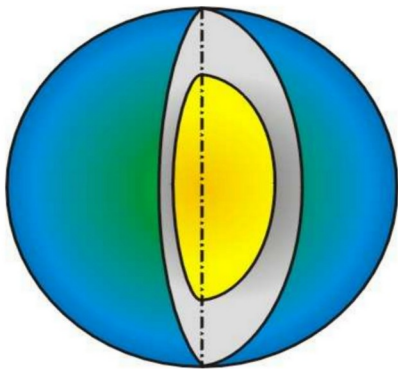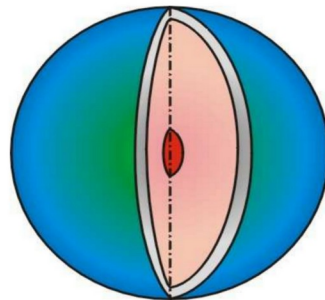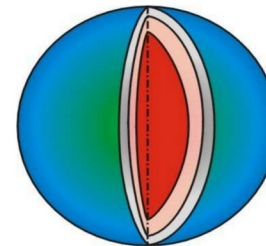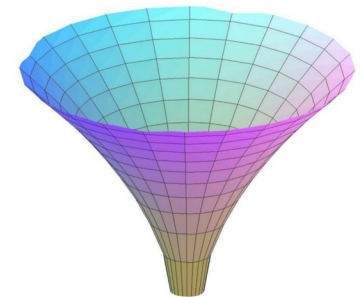
The Equation of State (EoS)

The construction of an realistic EoS, which includes a hadron-quark phase transition, depends on the underlying effective model of the hadron and quark interaction.
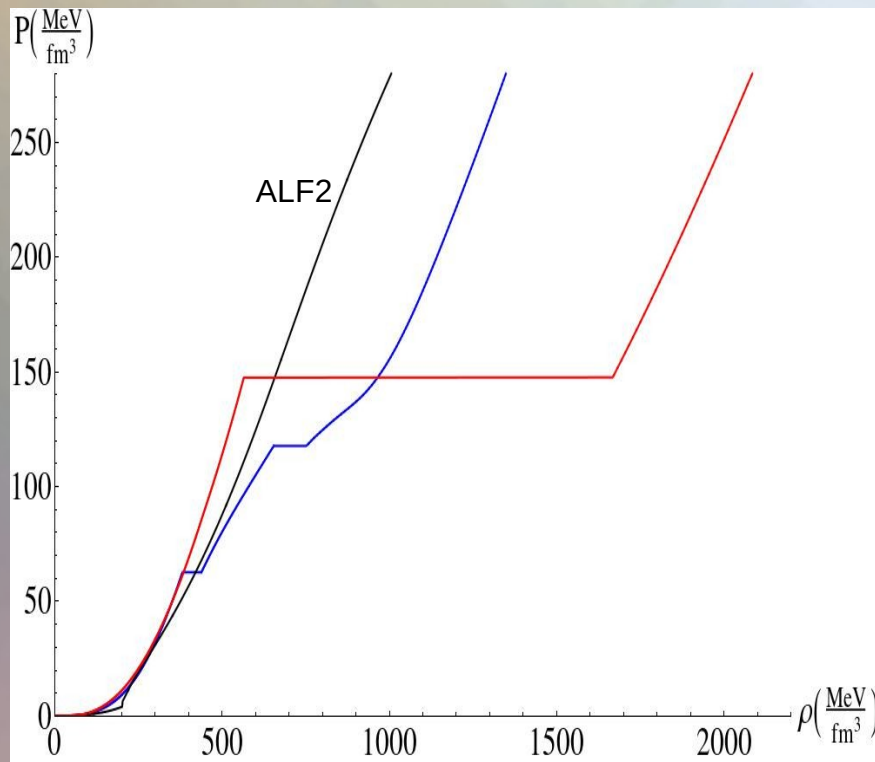
Selection of current EoS
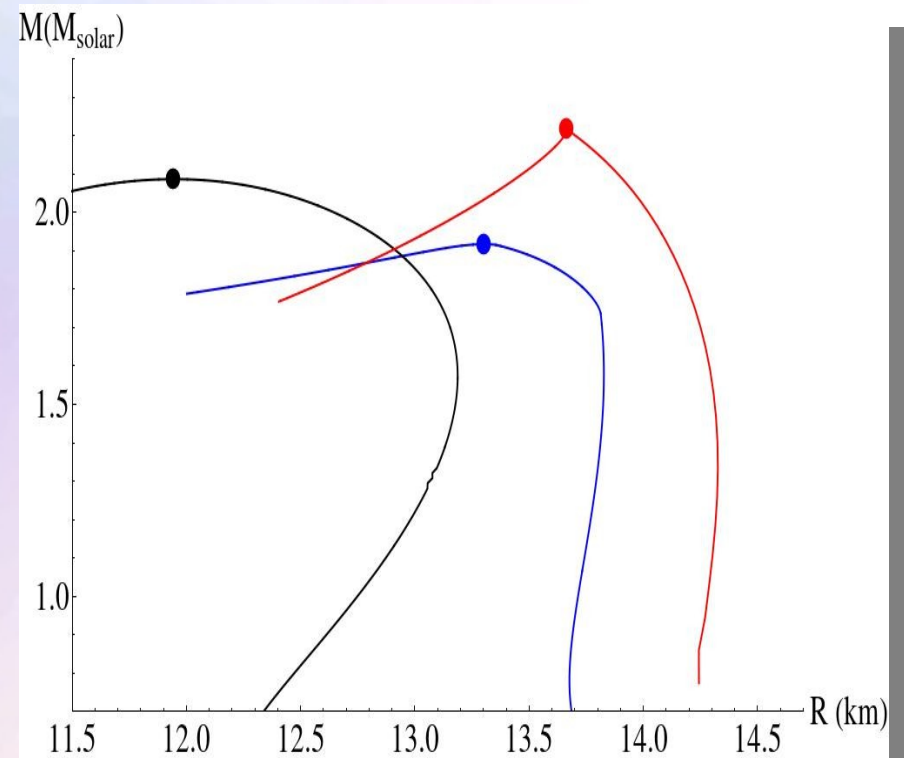
Star properties (Mass vs. Radius). Points correspond to the corresponding maximum mass of the EoS.

The Gibbs Construction

Hadronic and quark surface:
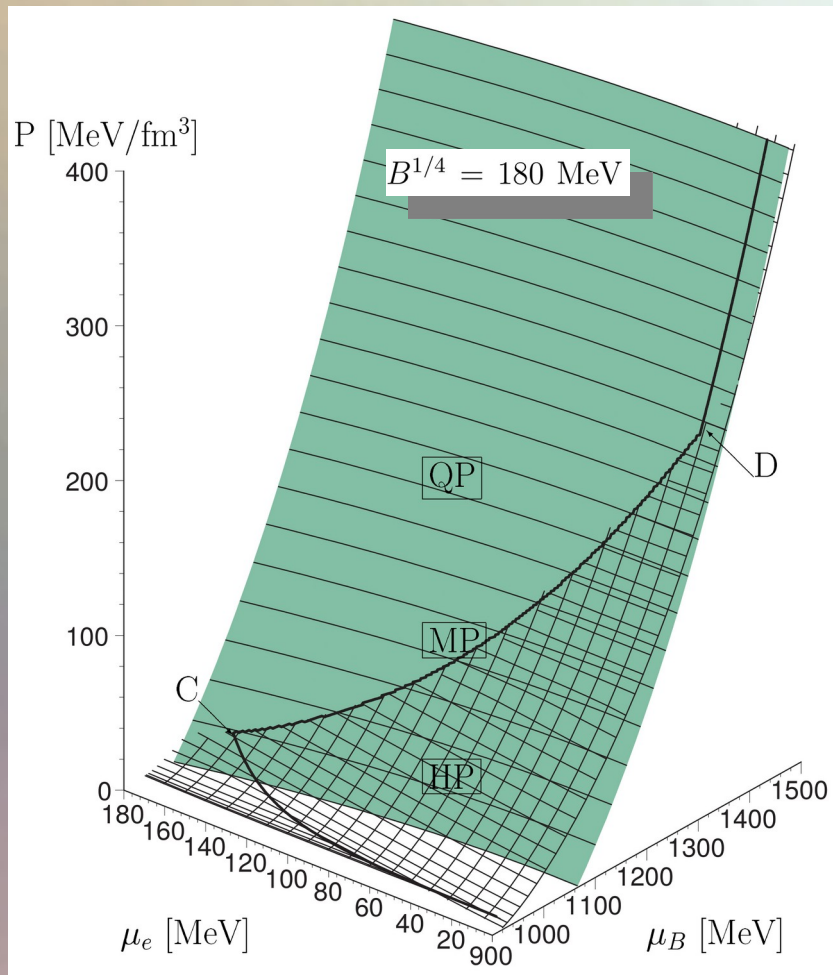
Charge neutrality condition is only globally realized

$$\rho_e := (1 - \chi)\rho_e^H(\mu_B, \mu_e) + \chi\rho_e^Q(\mu_B, \mu_e) = 0\,.$$
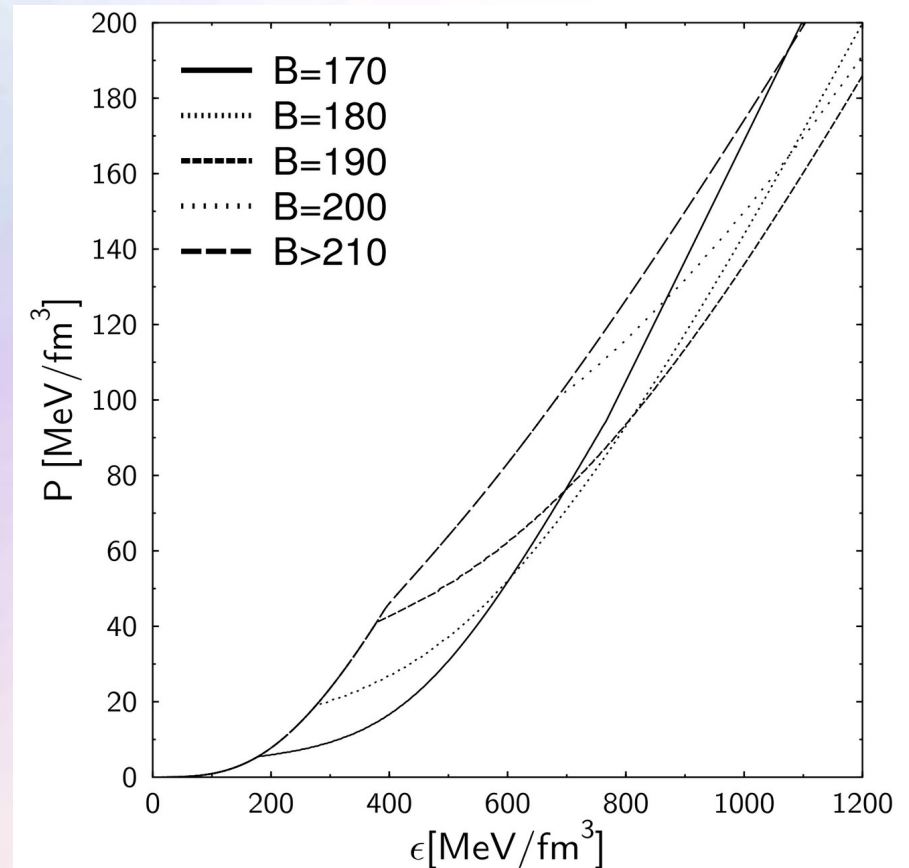
The Gibbs Construction

Hadronic and quark surface:
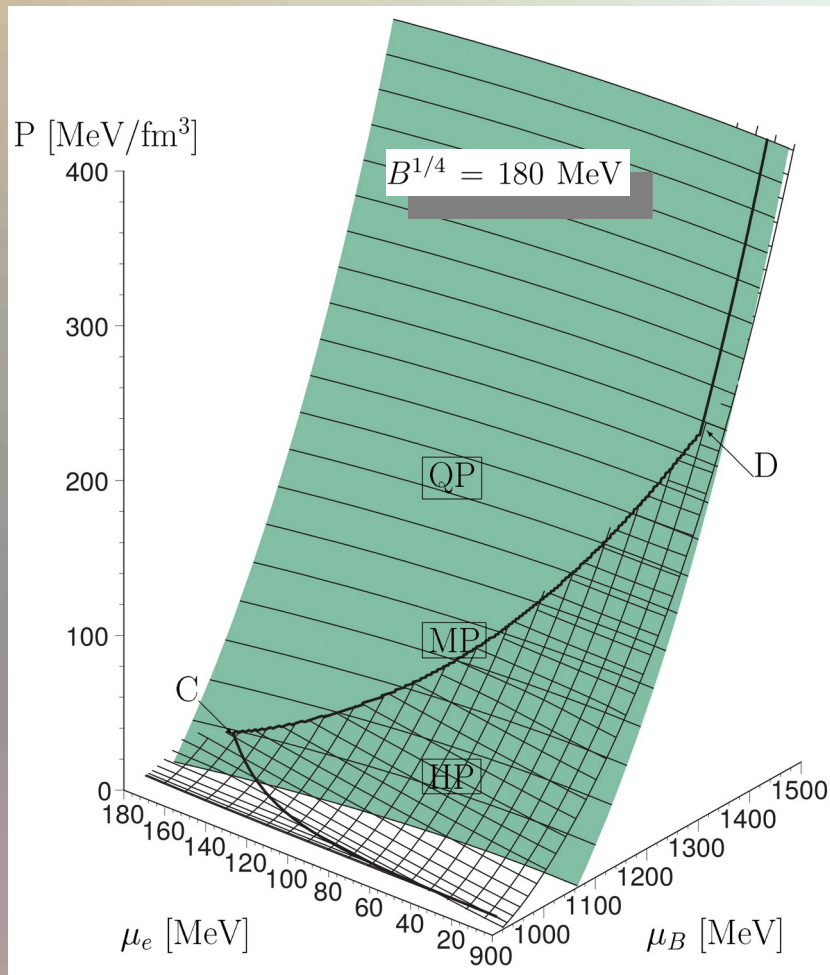
Particle composition:

$B^{1/4} = 180$ MeV
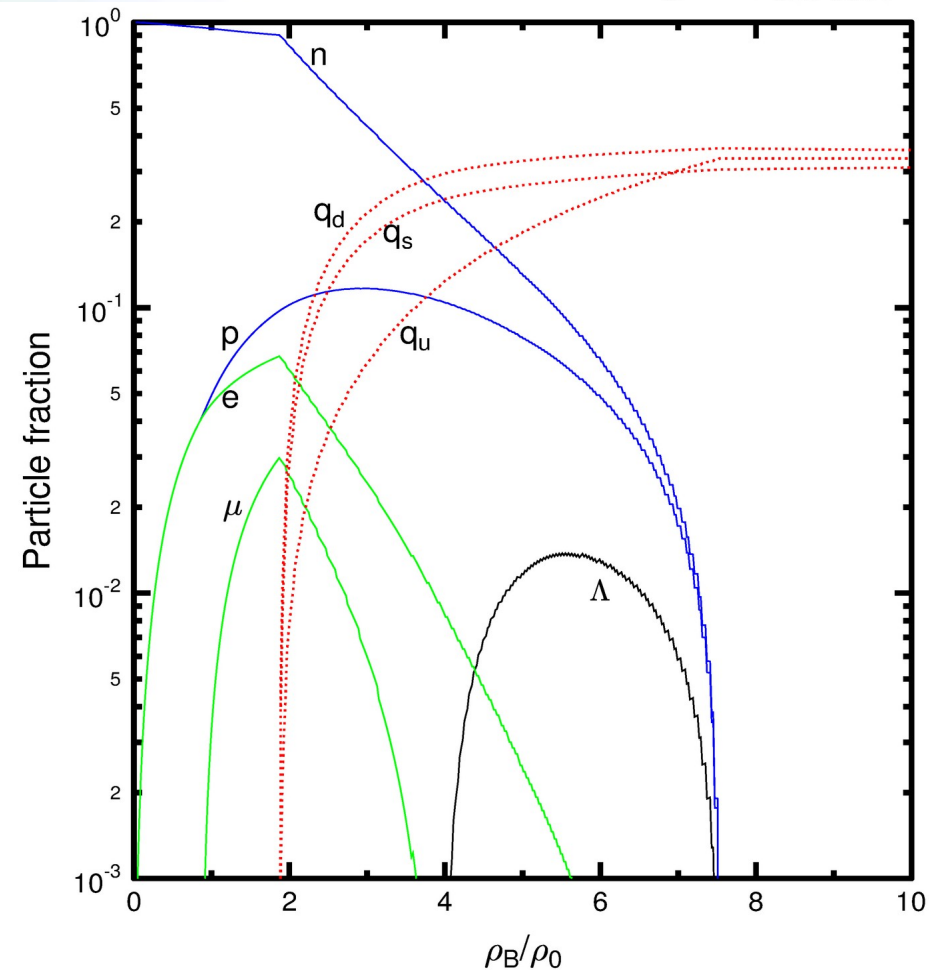
The Maxwell Construction

If the surface tension is large -> mixed phase disappears

-> sharp boundary between the hadron and quark phase -
>Maxwell construction should be used
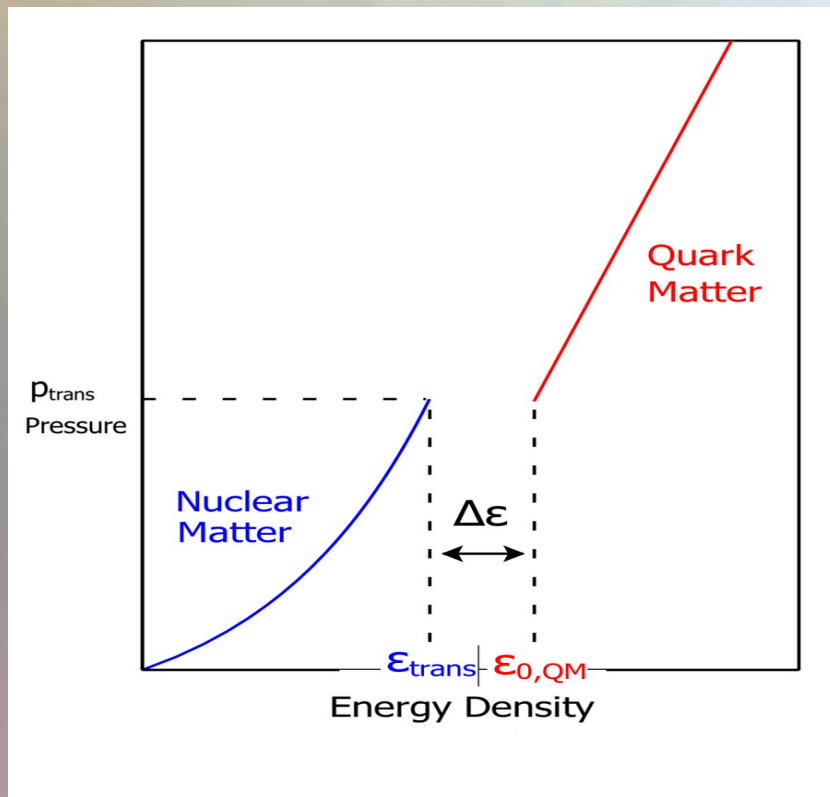
Image from M.G. Alford, S. Han, and M. Prakash, Phys. Rev. D 88, 083013 (2013)
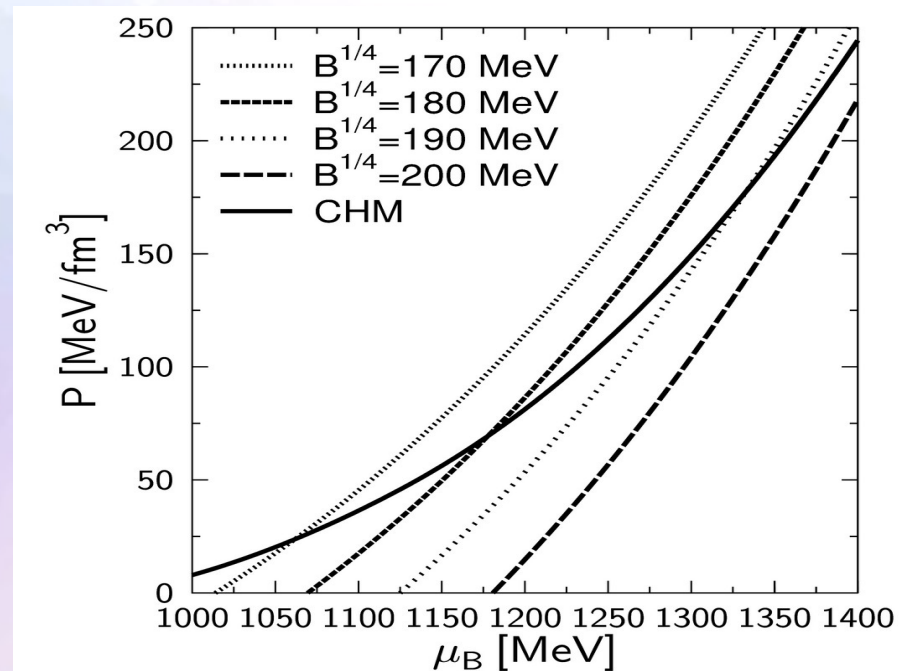
Pressure and baryon chemical potential stays constant, while the density and the charge chemical potential jump discontinuously during the phase transition.

Summary

- The transition from confined hadronic matter to deconfined quark matter is called the <u>Hadron-Quark Phase Transition</u>
- Depending on the value of the hadron-quark surface tension, the <u>Maxwell- or Gibbs-phase transition</u> construction should be used
- The star's density profile has a <u>huge density jump (Riemann problem)</u> at the phase transition boundary, if a Maxwell construction is used
- Realistic numerical simulations of collapsing neutron stars or neutron star mergers <u>should use an EoS with a hadron quark phase transition</u>
- <u>Realistic rotation profile in hyper massive neutron stars</u> indicate that the maximum of the rotation curve come along with the hadron quark phase transition boundary (mixed phase if Gibbs is used)
- The decisive amount of matter which is trapped behind the event horizon when a <u>black hole</u> is formed (in an merger or collapsing scenario of neutron stars) is deconfined quark matter

Current Projects

- The twin star collapse
  (Collaborators: A.Zacchi, J.Schaffner-Bielich and L.Rezzolla)

- Oscillations of hybrid and quark stars within different models of the phase transition
  (Collaborators: A.Brillante, I.Mishustin, A.Sedrakian and L.Rezzolla)

- Hybrid and quark star merger calculations with temperature dependent equation of states
  (Collaborators: S. Schramm, B.Franzon, F.Galeazzi and L.Rezzolla)

- Differential rotation profiles of hypermassive hybrid stars and the effect Maxwell- vs. Gibbs-construction
  (Collaborators: K.Takami, F.Galeazzi, B.Mundim, L.Bovard and L.Rezzolla)

- Collapse scenario and black hole formation in the context of the hadron-quark phase transition

Current Projects

- The twin star collapse
  (Collaborators: A.Zacchi, J.Schaffner-Bielich and L.Rezzolla)

- Oscillations of hybrid and quark stars within different models of the hadron-quark phase transition
  (Collaborators: A.Brillante, I.Mishustin, A.Sedrakian and L.Rezzolla)

- Hybrid and quark star merger calculations with temperature dependent equation of states
  (Collaborators: S. Schramm, B.Franzon, F.Galeazzi and L.Rezzolla)

- Differential rotation profiles of hypermassive hybrid stars and the effect Maxwell- vs. Gibbs-construction
  (Collaborators: K.Takami, F.Galeazzi, B.Mundim, L.Bovard and L.Rezzolla)

- Collapse scenario and black hole formation in the context of the hadron-quark phase transition

The Twin Star Collapse

Usually it is assumed that this loss of stability leads to the collapse into a black hole. However, realistic calculations open another possibility: the collapse into the twin star on the second sequence. A star from the first sequence which reaches the maximum mass (point A) will collapse to its twin star. The latter is the corresponding star on the second sequence, i.e. the one which has the same total baryon number (point B).

I.N. Mishustin, M. Hanauske, A. Bhattacharyya, L.M. Satarov, H. Stöcker, and W. Greiner, "Catastrophic rearrangement of a compact star due to quark core formation", Physics Letters B 552 (2003) p.1-8

J. Schaffner-Bielich, M. Hanauske, H. Stöcker, and W. Greiner, Phys. Rev. Lett. 89, 171101 (2002)

S. Banik, M. Hanauske, D. Bandyopadhyay, and W. Greiner, Phys. Rev. D 70, 123004 (2004)
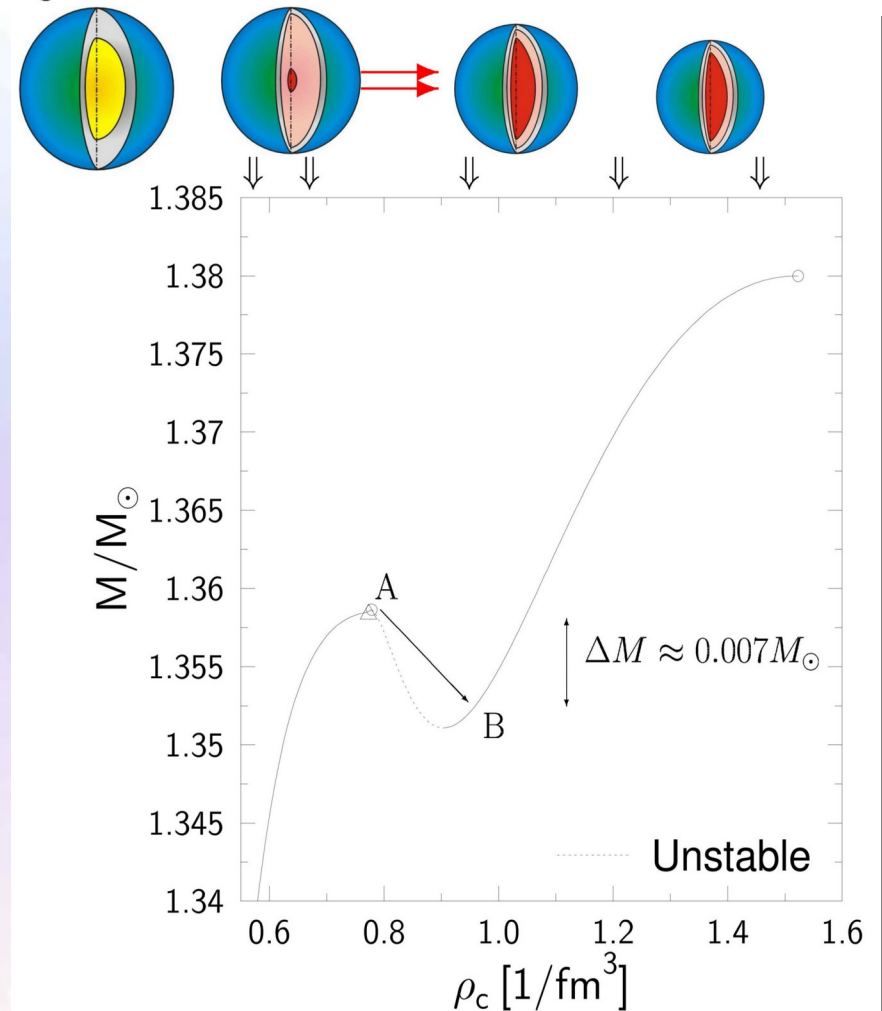
The Twin Star Collapse

Density profiles of the two twins
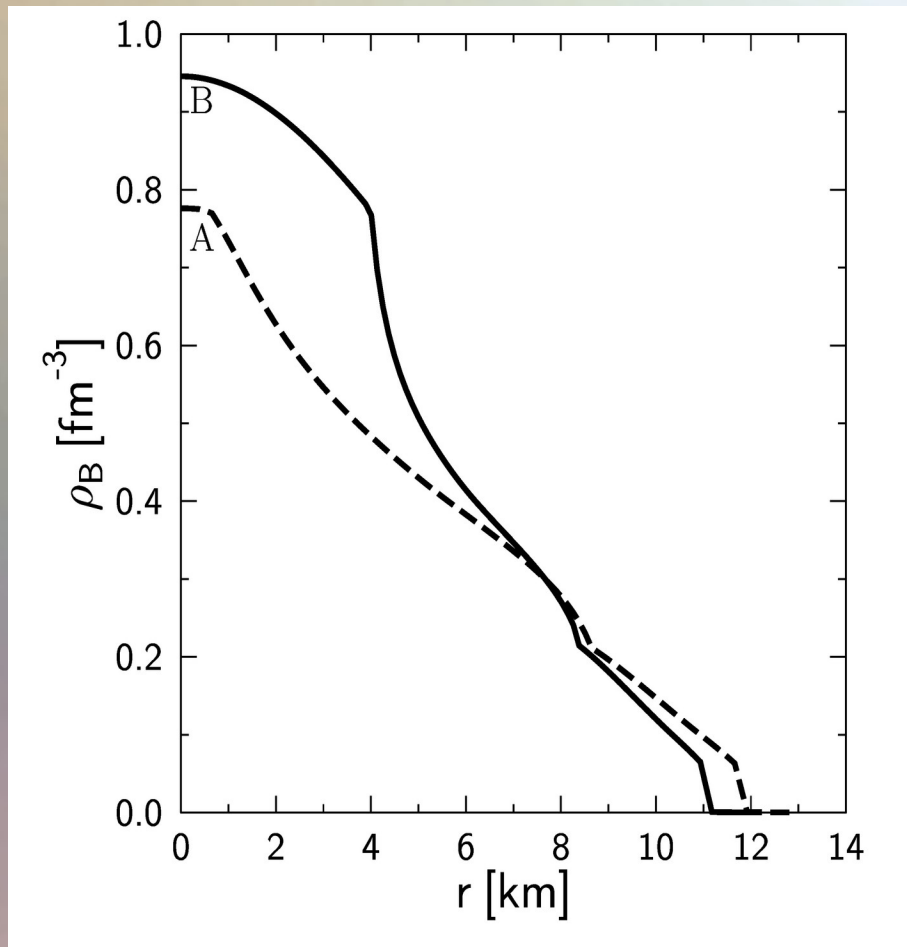
Conservation of total baryonic mass
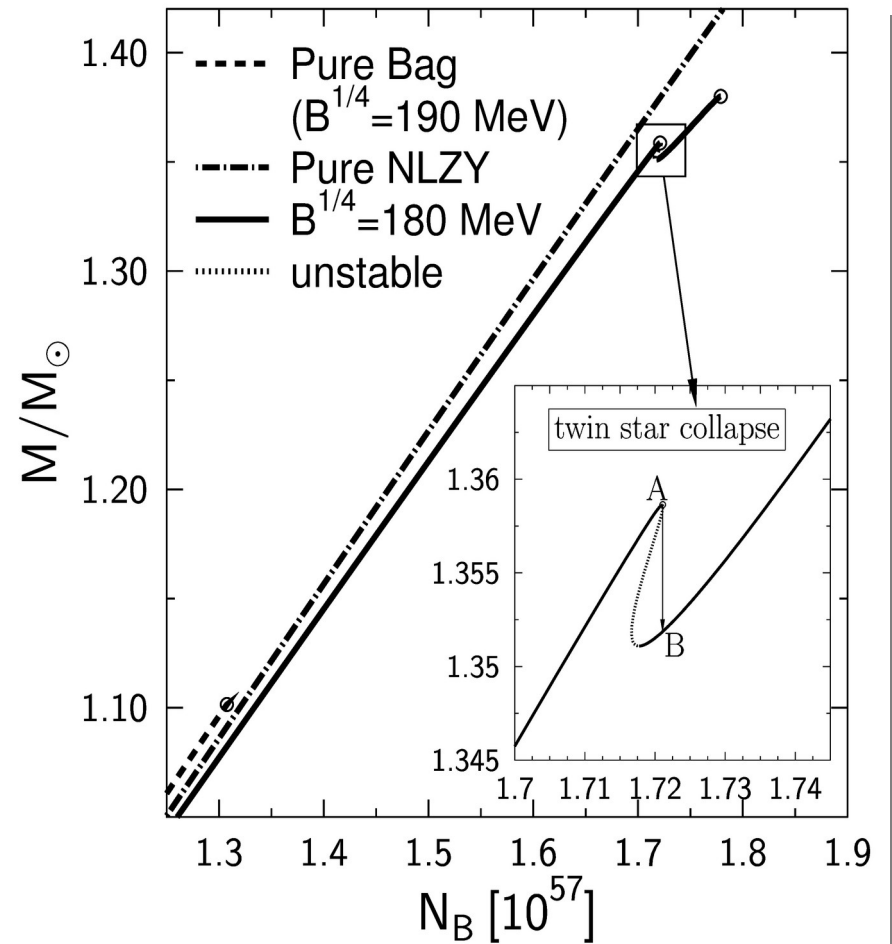
Summary

- The transition from confined hadronic matter to deconfined quark matter is called the <u>Hadron-Quark Phase Transition</u>
- Depending on the value of the hadron-quark surface tension, the <u>Maxwell- or Gibbs-phase transition</u> construction should be used
- The star's density profile has a <u>huge density jump (Riemann problem)</u> at the phase transition boundary, if a Maxwell construction is used
- In a narrow parameter window <u>Twin Stars</u> a possible: The collapse from a neutron to a hybrid quark star will emit a burst of gravitational waves, neutrinos and gamma rays
- Realistic numerical simulations of collapsing neutron stars or neutron star mergers <u>should use an EoS with a hadron quark phase transition</u>
- The decisive amount of matter which is trapped behind the event horizon when a <u>black hole</u> is formed (in an merger or collapsing scenario of neutron stars) is deconfined quark matter

Current Projects

- The twin star collapse
  (Collaborators: A.Zacchi, J.Schaffner-Bielich and L.Rezzolla)

- Oscillations of hybrid and quark stars within different models of the hadron-quark phase transition
  (Collaborators: A.Brillante, I.Mishustin, A.Sedrakian and L.Rezzolla)

- Hybrid and quark star merger calculations with temperature-dependent equation of states
  (Collaborators: S. Schramm, B.Franzon, F.Galeazzi and L.Rezzolla)

- Differential rotation profiles of hypermassive hybrid stars and the effect Maxwell- vs. Gibbs-construction
  (Collaborators: K.Takami, F.Galeazzi, B.Mundim, L.Bovard and L.Rezzolla)

- Collapse scenario and black hole formation in the context of the hadron-quark phase transition

Collapse Scenario of a Hybrid Star

The gravitational collapse of a hybrid star to a black hole is visualized on the right side within a space-time diagram of the Schwarzschild metric in advanced Eddington-Finkelstein coordinates.

The formation of the apparent and event horizon of the black hole confines the quark star macroscopically. Finally the colour charge of the deconfined free quarks cannot be observed from outside.

M. Hanauske, Dissertation: "Properties of Compact Stars within QCD-motivated Models" ;
University Library Publication 2004 (urn:nbn:de:hebis:30-0000005872)
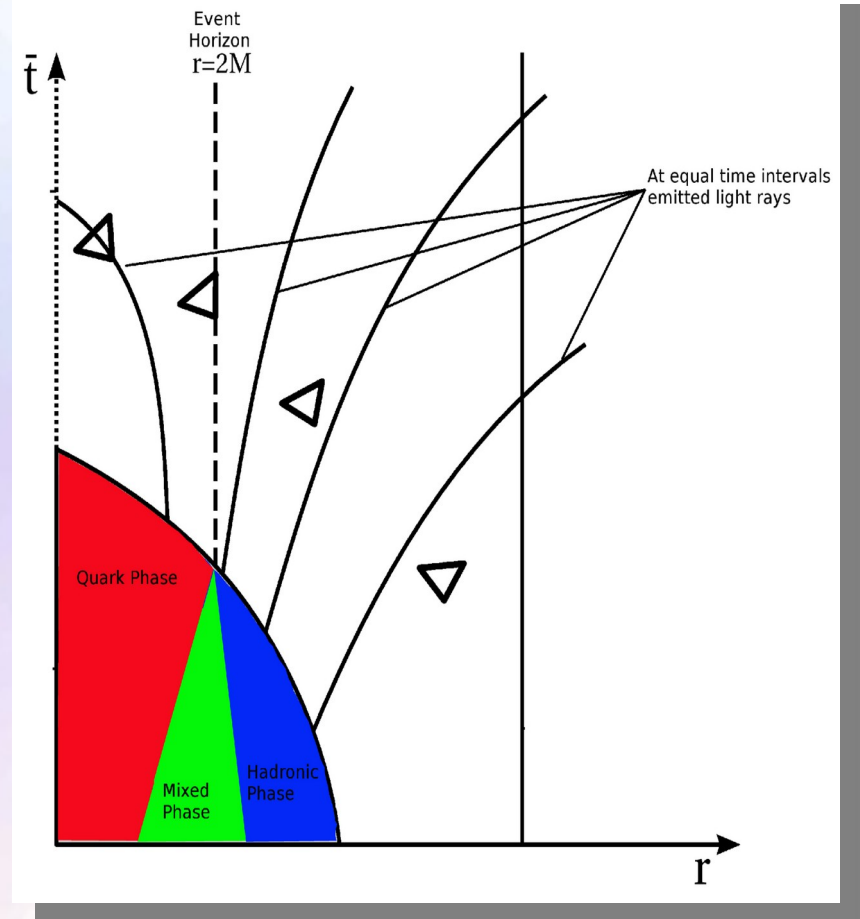
The QCD- Phase Diagram

The QCD phase diagram at temperature T and net baryon density is displayed on the right side.

Some regions can be accessed by heavy ion collisions at different energies.

Matter of the early universe and in the interior of compact stars are also indicated within the diagram.

Image from
http://webarchiv.fz-juelich.de/nic/Publikationen/Broschuere/
Elementarteilchenphysik/hadron.jpg
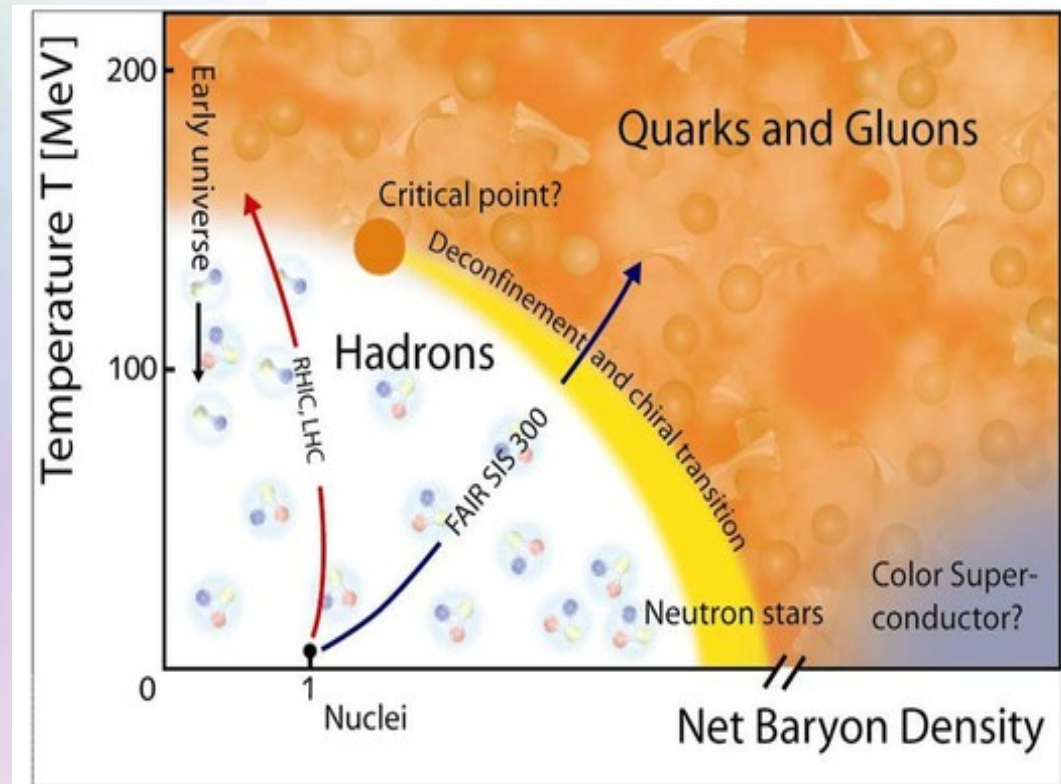
The QCD- Phase Diagram II
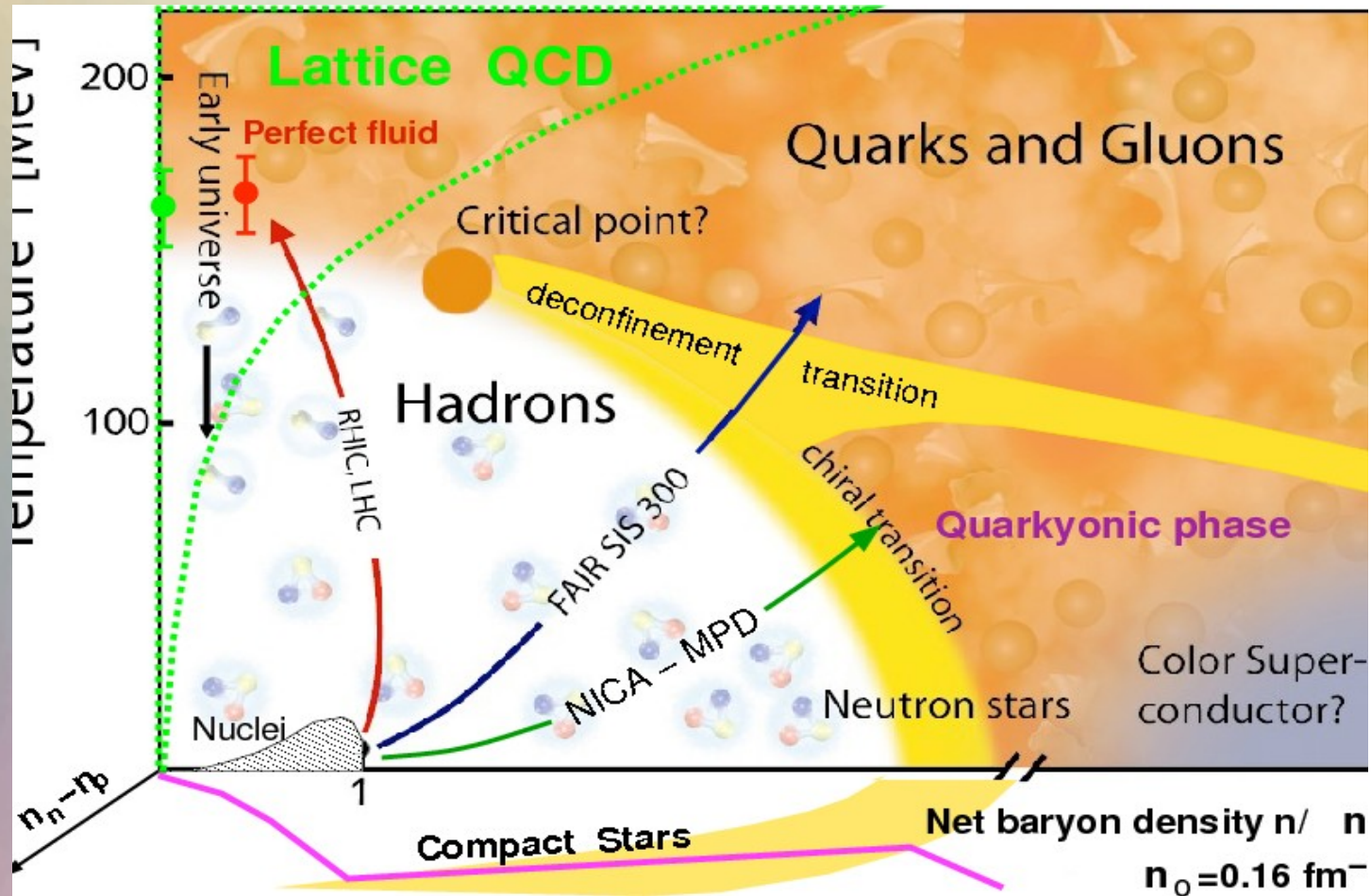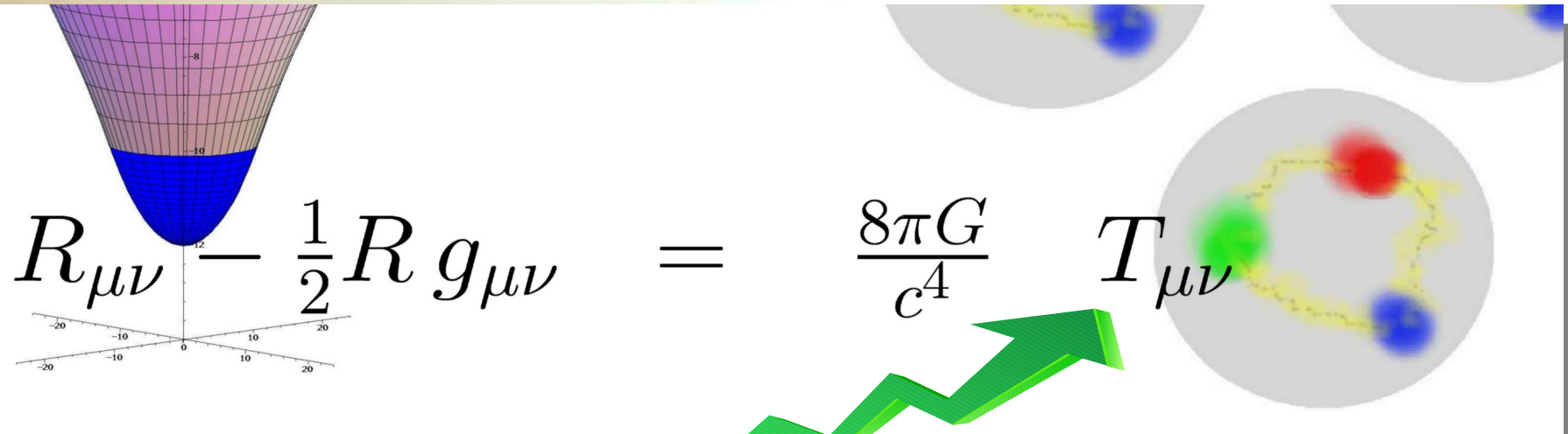
Image from http://inspirehep.net/record/823172/files/phd_qgp3D_quarkyonic2.png

Neutron Stars (NS)

$$R_{\mu\nu} - \frac{1}{2}R\,g_{\mu\nu} \;=\; \frac{8\pi G}{c^4}\,T_{\mu\nu}$$

Relativistic Mean-Field Hadronic Models

$$\sum_B \; (p, n, \Lambda, \Sigma^-, \; \Sigma^0, \Sigma^+, \Xi^-, \Xi^0)$$

$$\mathcal{L} \;=\; \sum_B \overline{\psi}_B \left(i\slashed{\partial} - m_B\right)\psi_B + \frac{1}{2}\partial^\mu\sigma\partial_\mu\sigma - \frac{1}{2}m_\sigma^2\sigma^2 - \frac{a}{3}\sigma^3 - \frac{b}{4}\sigma^4 - \frac{1}{4}\omega^{\mu\nu}\omega_{\mu\nu}$$

$$+ \frac{1}{2}m_\omega^2\omega^\mu\omega_\mu - \frac{1}{4}\vec{\rho}^{\,\mu\nu}\vec{\rho}_{\mu\nu} + \frac{1}{2}m_\rho^2\vec{\rho}^{\,\mu}\vec{\rho}_\mu + \sum_B \overline{\psi}_B \left(g_{\sigma B}\sigma + g_{\omega B}\omega^\mu\gamma_\mu + g_\rho\vec{\rho}^{\,\mu}\gamma_\mu\vec{\tau}_B\right)\psi_B$$

$$\mathcal{L}^{YY} \;=\; \frac{1}{2}\left(\partial^\mu\sigma^*\partial_\mu\sigma^* - m_{\sigma^*}^2\sigma^{*2}\right) - \frac{1}{4}\phi^{\mu\nu}\phi_{\mu\nu} + \frac{1}{2}m_\phi^2\phi^\mu\phi_\mu$$

$$+ \sum_Y \overline{\psi}_Y \left(g_{\sigma^* Y}\sigma^* + g_{\phi Y}\phi^\mu\gamma_\mu\right)\psi_Y \quad,$$

$$\mathcal{L}_{\text{lep}} \;=\; \sum_{l=e,\mu} \overline{\psi}_l [i\gamma_\mu\partial^\mu - m_l]\psi_l$$
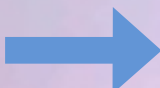
Composition of Neutron Star Matter

Neutron star matter conditions:

1) Charge Neutrality
2) β-equilibrium
3) Strangeness production

$$n \iff p + e + \tilde{\nu}_e$$

Λ-Hyperon $\quad n + n \leftrightarrow n + \Lambda + K^0 \quad \mu_\Lambda = \mu_n$

Σ^--Hyperon $\quad n + n \leftrightarrow n + \Sigma^- + K^+ \quad \mu_{\Sigma^-} = \mu_n + \mu_e$

Chemical potentials and single particle energies of hyperons in dependence of the baryonic density.

$$E_i(k) = E_i^*(k) + g_{i\omega}\omega_0 + g_{i\phi}\phi_0 + g_{i\rho}I_{3i}\rho_0$$

$$E_i^*(k) = \sqrt{k_i^2 + m_i^{*2}} \qquad \mu_i = b_i\mu_n - q_i\mu_e$$

M. Hanauske, D. Zschiesche, S. Pal, S. Schramm, H. Stöcker, and W. Greiner, Astrophys. J. 537, 958 (2000)

Particle composition vs baryonic density
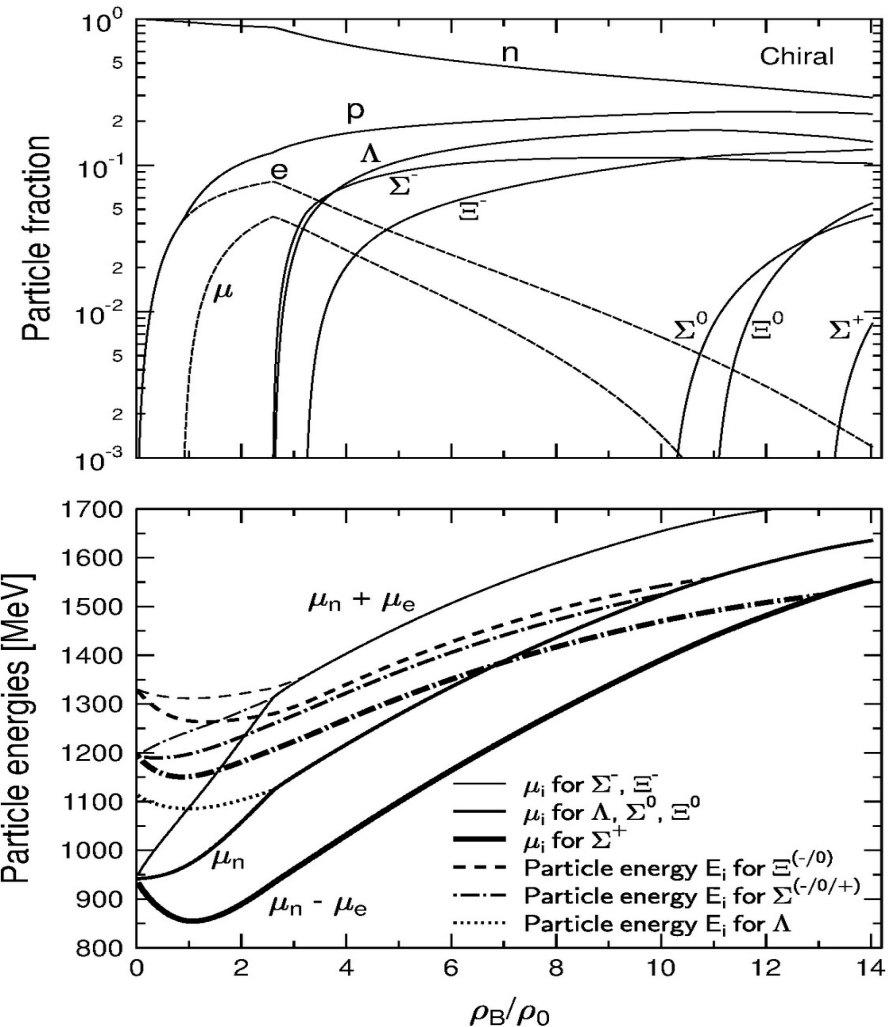
Neutron Star Properties

The neutron star radius as a function of its mass. A low, middle and high density star is displayed within the figure. Additionally the onset of hyperonic particles is visualized.
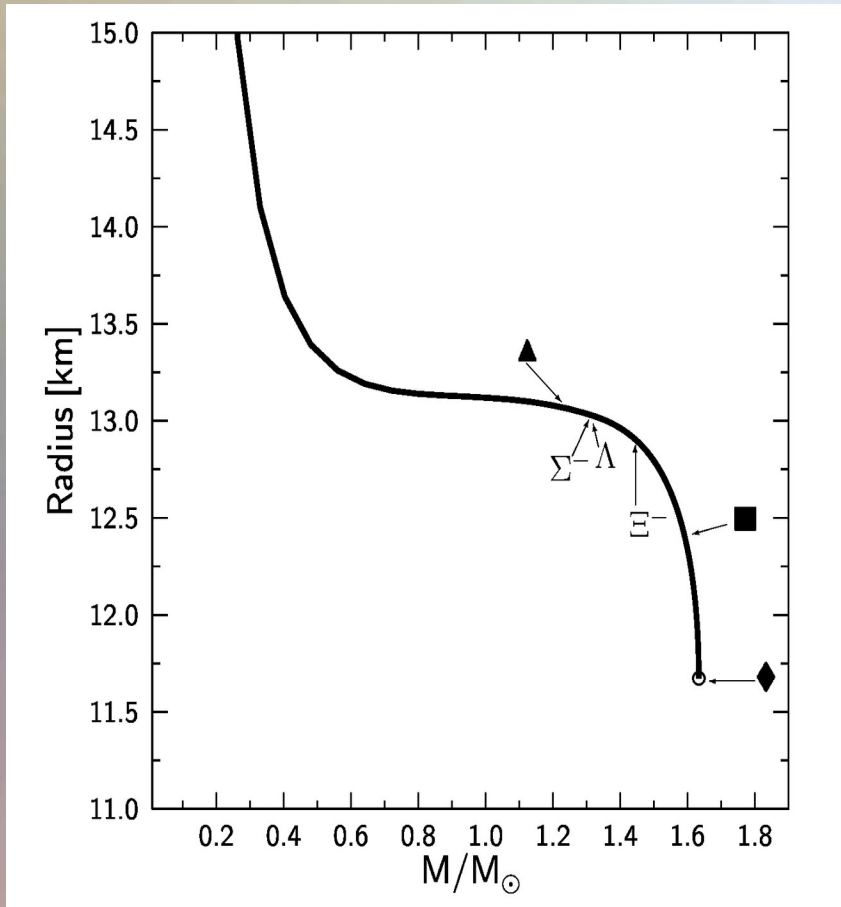
Energy density profiles of three neutron stars with different central densities and masses. The low density stars do not contain any hyperons, whereas the other two stars do have hyperons in their inner core.
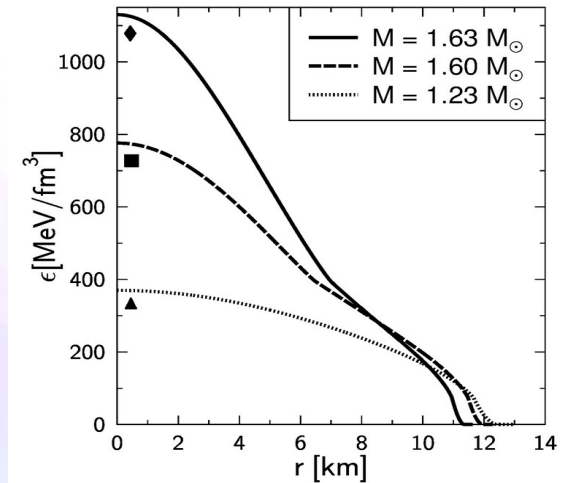
Time-time component of the metric tensor as a function of the radial coordinate. The solid line corresponds to the inner TOV-solution, whereas the doted curve depicts the outer Schwarzschild part.

Hybrid Stars

$$R_{\mu\nu} - \frac{1}{2} R\, g_{\mu\nu} \;=\; \frac{8\pi G}{c^4}\; T_{\mu\nu}$$
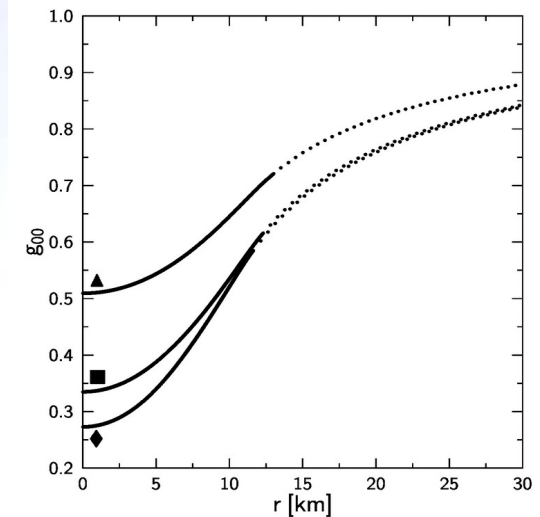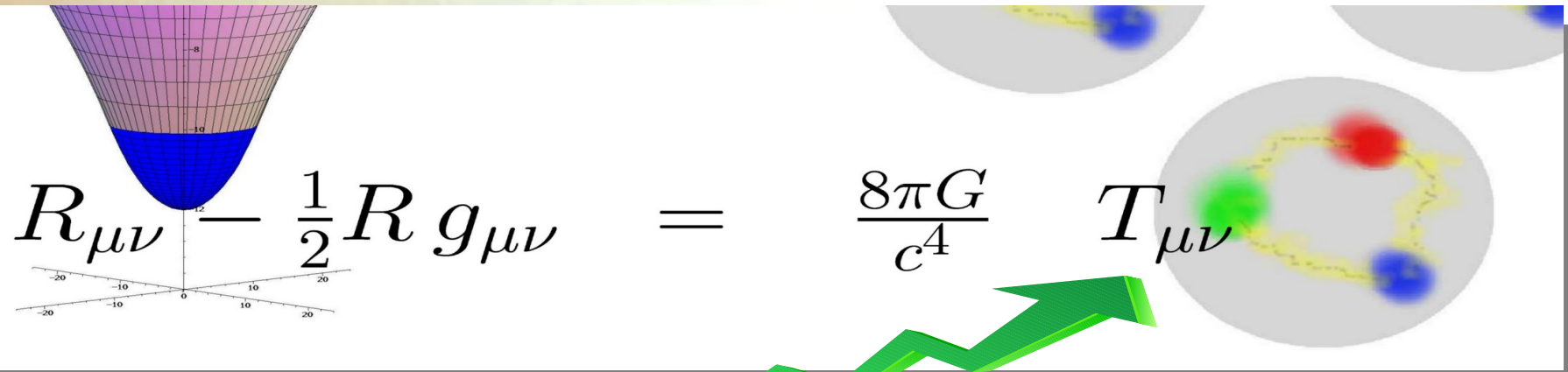
Hadronic Model + Quark Model (eg. NJL model or MIT-Bag model)

Lagrangian density of the NJL model

$$\mathcal{L} \;=\; \underbrace{\overline{\psi}\,(i\,\partial\!\!\!/ - \hat{m}_0)\,\psi}_{\text{Kinetische und Massenbeiträge}} \;+\; \underbrace{G_S \sum_{j=0}^{8} \left[\left(\overline{\psi}\,\frac{\lambda_j}{2}\,\psi\right)^2 + \left(\overline{\psi}\,\frac{i\gamma_5\lambda_j}{2}\,\psi\right)^2\right]}_{\text{Skalare Wechselwirkung}}$$

$$\underbrace{-\,G_V \sum_{j=0}^{8}\left[\left(\overline{\psi}\,\gamma_\mu\frac{\lambda_j}{2}\,\psi\right)^2 + \left(\overline{\psi}\,\gamma_\mu\frac{\gamma_5\lambda_j}{2}\,\psi\right)^2\right]}_{\text{Vektorielle Wechselwirkung}} \qquad \psi \;\equiv\; \psi_{Aa}^{f}$$

$$\underbrace{-\,K\left[\det_f\left(\overline{\psi}\,(1-\gamma_5)\,\psi\right) + \det_f\left(\overline{\psi}\,(1+\gamma_5)\,\psi\right)\right]}_{\text{Flavour Mischterme}} + \underbrace{\mathcal{L}_L}_{\text{Leptonische Beiträge}}$$

MIT-Bag model

$$\epsilon^Q \;=\; \sum_{f=u,d,s} \frac{\nu_f}{2\pi^2} \int_0^{k_F^f} k^2 \sqrt{m_f^2 + k^2}\, dk \;+\; B$$

$$P^Q \;=\; \sum_{f=u,d,s} \frac{\nu_f}{6\pi^2} \int_0^{k_F^f} \frac{k^4}{\sqrt{m_f^2 + k^2}}\, dk \;-\; B,$$

The Gibbs Construction

Hadronic and quark surface:

Particle composition:

$B^{1/4} = 200$ MeV
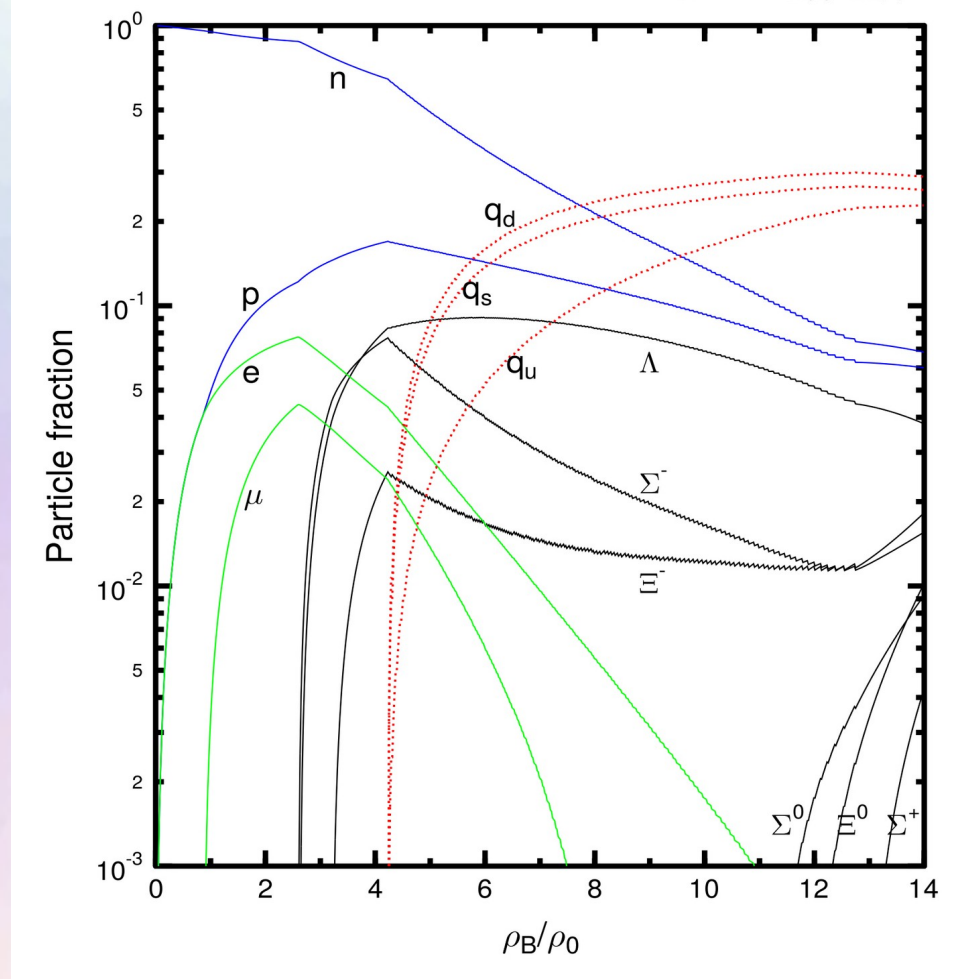
M. Hanauske, Dissertation, "Properties of Compact Stars within QCD-motivated Models"

Hybrid Star Properties

In contrast to the Gibbs construction, the star's density profile within the Maxwell construction (see right figure) will have a huge density jump at the phase transition boundary. Twin star properties can be found more easily when using a Maxwell construction.

Mass-Density relation

Energy-density profiles

Matthias Hanauske: "How to detect the QGP with telescopes", GSI Annual Report 2003, p.96
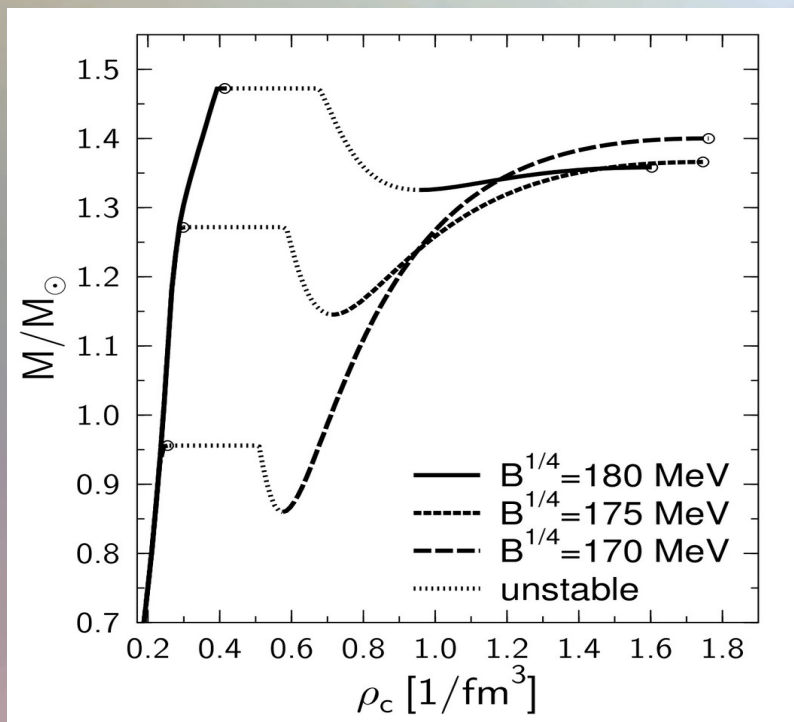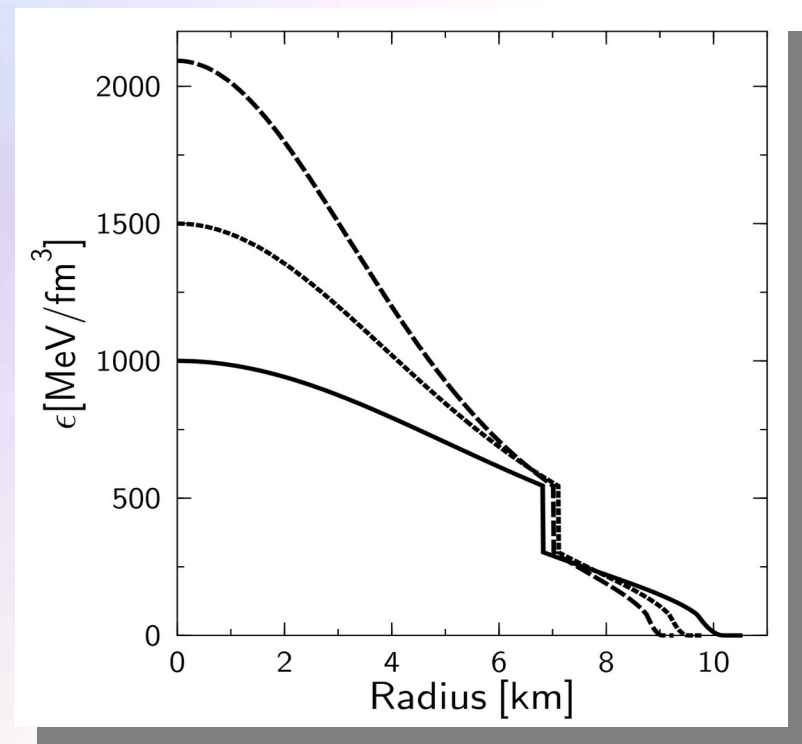
Observed Masses of Compact Star Binaries

PSR J1906+0746
Van Leeuwen et al, arXiv:1411.1518

144-ms pulsar, discovered in in 2004
Orbital period: 3.98 hours, Eccentricity: 0.085
Pulsar mass: 1.291(11), Companion mass 1.322(11)
Observed between 1998-2009,
then it disappeared due to spin precession

Double Pulsar PSR J0737-3039

Orbital period: 147 min, Eccentricity: 0.088
pulsar A: P=23 ms, M=1.3381(7)
pulsar B: P=2.7 s, M=1.2489(7)
Pulsar A is eclipsed once per orbit by B (for 30 s)
Kramer, Wex, Class. Quantum Grav. 2009

PSR J0348+0432

Orbital Period:
2.46 hours

Pulsar mass:
2.01+-0.04

white dwarf mass:
0.172+-0.003
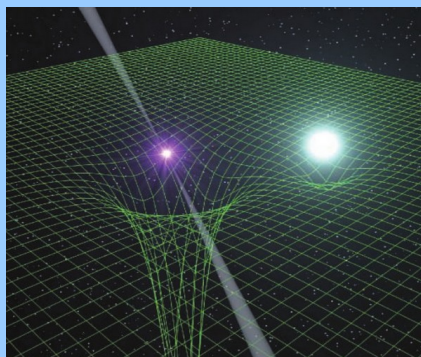
Picture from J. Antoniadis et.al. Science 2013

updated 15 January 2014

X-ray/Optical binaries

black widow pulsar
bwp

double neutron star binaries
Hulse-Taylor binary
in M15
double pulsar
in NGC 6544

white dwarf-neutron star binaries
in NGC 6539
in Ter 5
in 47 Tuc
in NGC 1851
in M 5
in NGC 6440
in NGC 6441
in NGC 6752
in NGC 6544
triple system w 2 WD

main sequence-neutron star binaries

Neutron star mass (M⊙)

Summary: Neutron Stars

Schematic Structure of a Neutron Star

Outer Envelopes

The outer envelopes of a neutron star constist of a thin plasma atmosphere where the thermal radiation is formed and a outer and inner crust which consist of electrons and nuclei. The whole outer envelope is about one kilometer thick and it occupies the density range $\epsilon \leq 0.5\,\epsilon_0$.
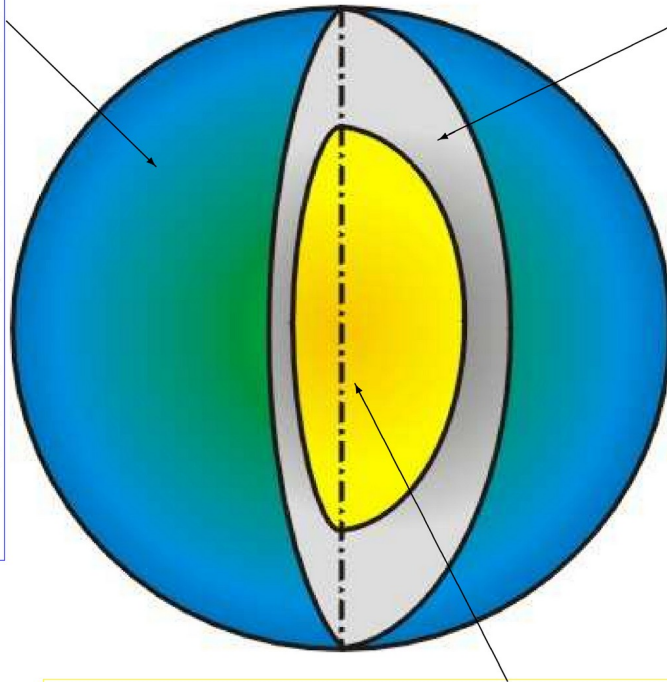
Outer Core

The outer core consists mainly of neutrons with several per cent admixture of protons, electrons and myons. It is several kilometers thick and occupies the density range $0.5\,\epsilon_0 < \epsilon \leq 2\,\epsilon_0$.

Nuclear matter density:
$\epsilon_0 = 2.8 \cdot 10^{14}\ \mathrm{g/cm^3}$

Inner Core

In the inner core of a neutron star hyperonic particles ($\Sigma^-, \Lambda, \Xi...$) are present. The inner core extends to the center of the star where its central density can be as high as $\epsilon \approx 15\,\epsilon_0$.

Neutron Star Matter
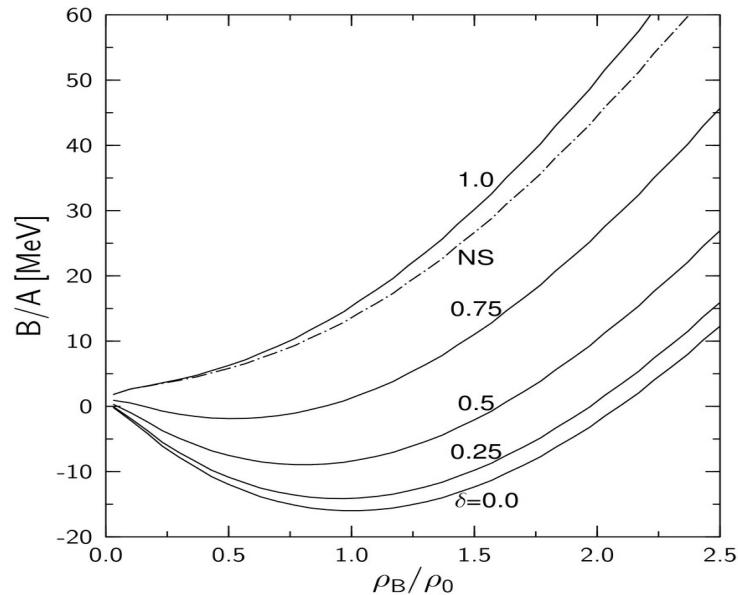
Binding energy per nucleon as a function of the baryonic density for different values of the neutron-proton asymmetry δ. 'NS' describes charge-neutral neutron star matter in β-equilibrium.

1) The equation of state (pressure P of the hadronic matter vs. the baryonic density). The solid curve (npe) describes charge-neutral matter in β-equilibrium consisting of neutrons, protons and electrons, whereas the dotted curve (npeμY) includes muons and hyperons.

In contrast to normal nuclear matter, neutron star matter needs to fulfil three additional conditions:

1) Charge Neutrality

2) β-equilibrium $\quad n \;\Leftrightarrow\; p + e + \tilde{\nu}_e$

3) Strangeness production

$$N + N \;\Rightarrow\; N + H + M \;,$$
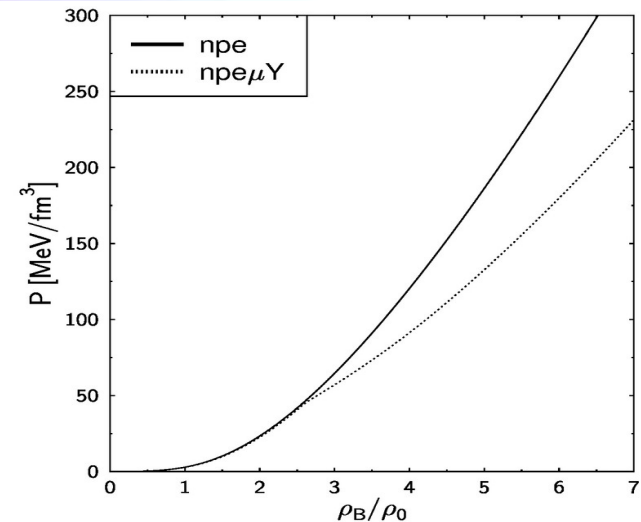
Hybrid Stars

To describe the properties of the Hadron-Quark phase transition happening in Hybrid stars an effective model for the quark phase is needed:

$$\lambda_j \equiv \lambda_{ja}{}^b$$

$$\mathcal{L} = \underbrace{\overline{\psi}\,(i\,\partial\!\!\!/ - \hat{m}_0)\,\psi}_{\text{Kinetische und Massenbeiträge}} + \underbrace{G_S \sum_{j=0}^{8} \left[\left(\overline{\psi}\,\frac{\lambda_j}{2}\,\psi \right)^2 + \left(\overline{\psi}\,\frac{i\gamma_5\lambda_j}{2}\,\psi \right)^2 \right]}_{\text{Skalare Wechselwirkung}}$$

$$\underbrace{-\, G_V \sum_{j=0}^{8} \left[\left(\overline{\psi}\,\gamma_\mu\frac{\lambda_j}{2}\,\psi \right)^2 + \left(\overline{\psi}\,\gamma_\mu\frac{\gamma_5\lambda_j}{2}\,\psi \right)^2 \right]}_{\text{Vektorielle Wechselwirkung}} \qquad \psi \equiv \psi^f_{Aa}$$

$$\partial\!\!\!/ \equiv \partial\!\!\!/_A{}^B := \partial_\mu \gamma^\mu{}_A{}^B$$

$$\underbrace{-\, K \left[\det_f \left(\overline{\psi}\,(1 - \gamma_5)\,\psi \right) + \det_f \left(\overline{\psi}\,(1 + \gamma_5)\,\psi \right) \right]}_{\text{Flavour Mischterme}} + \underbrace{\mathcal{L}_L}_{\text{Leptonische Beiträge}}$$

Eg. the Nambu-Jona-Lasinio (NJL) Model or the
MIT-Bag model

$$\epsilon^Q = \sum_{f=u,d,s} \frac{\nu_f}{2\pi^2} \int_0^{k_F^f} k^2 \sqrt{m_f^2 + k^2}\, dk\ + B$$

$$P^Q = \sum_{f=u,d,s} \frac{\nu_f}{6\pi^2} \int_0^{k_F^f} \frac{k^4}{\sqrt{m_f^2 + k^2}}\, dk\ - B\,,$$

A hybrid model of a compact star is realized by a construction of a phase transition between a hadronic model and a quark model. In contrast to the Maxwell construction of a phase transition, in a Gibbs construction a mixed phase is present in the stars interior, where both phases co-exist. In the mixed phase transition region each phase has a charge; only the overall electrical charge density vanishes. In the mixed phase, the pressure of the hadronic matter has to be equal to the pressure of the quark phase, whereas the particle and energy densities differ.

The Gibbs Construction

Since the charge neutrality condition is only globally realized, the pressure depends on two independently chemical potentials, the baryonic and charge chemical potential:

$$\begin{aligned} P^H(\mu_B, \mu_e) &= P^Q(\mu_B, \mu_e), \\ \mu_B = \mu_B^H &= \mu_B^Q, \\ \mu_e = \mu_e^H &= \mu_e^Q \end{aligned}$$

Charge density neutrality condition:

$$\rho_e := (1 - \chi)\rho_e^H(\mu_B, \mu_e) + \chi\rho_e^Q(\mu_B, \mu_e) = 0.$$
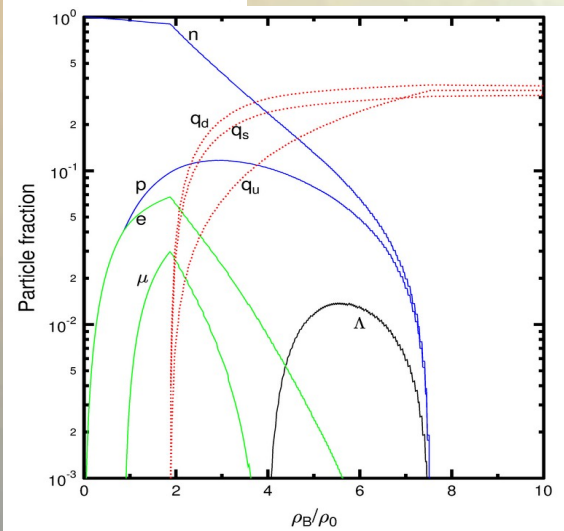
Overall baryonic density:

$$\rho_B = (1 - \chi)\rho_B^H(\mu_B, \mu_e) + \chi\rho_B^Q(\mu_B, \mu_e),$$

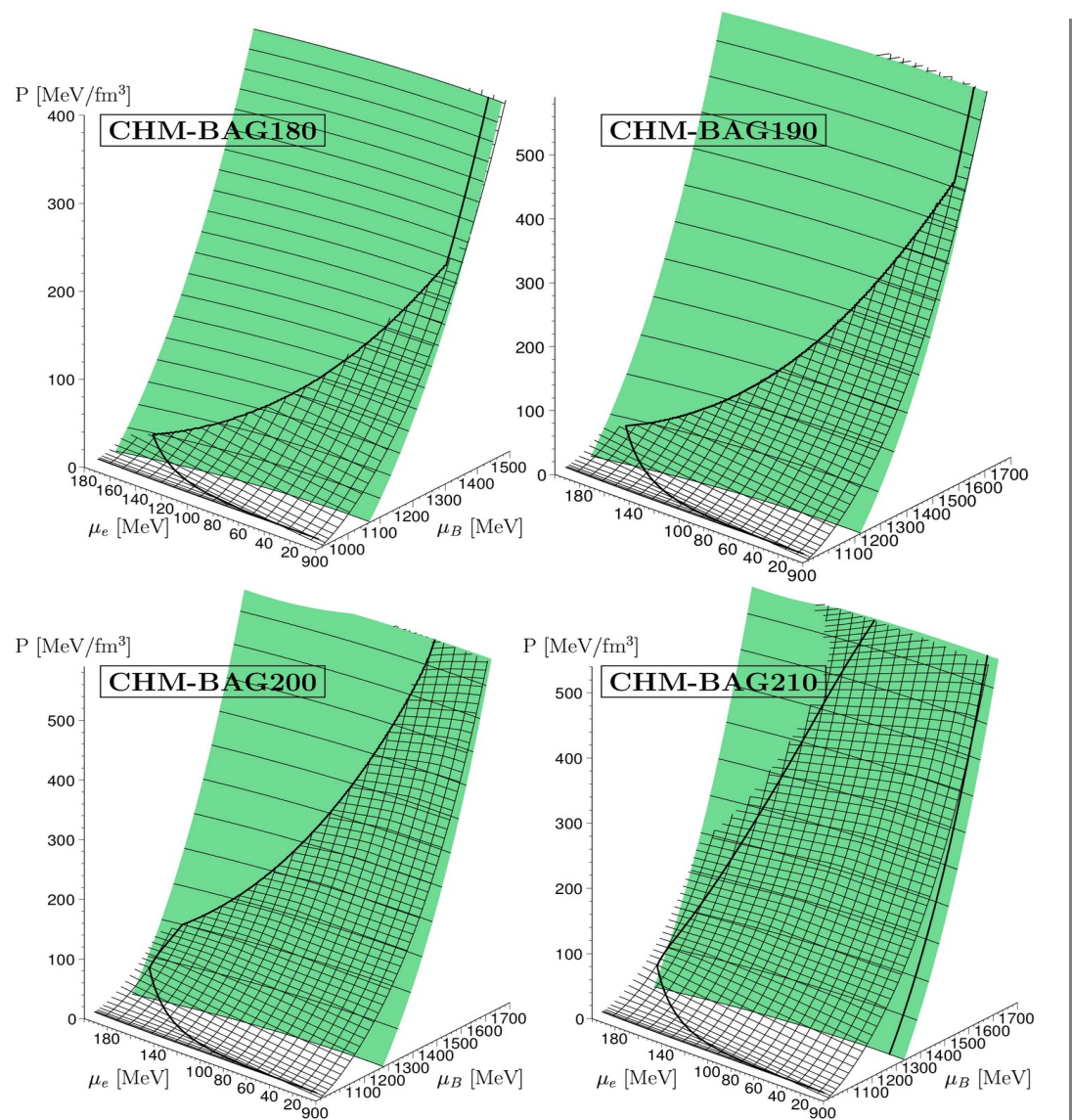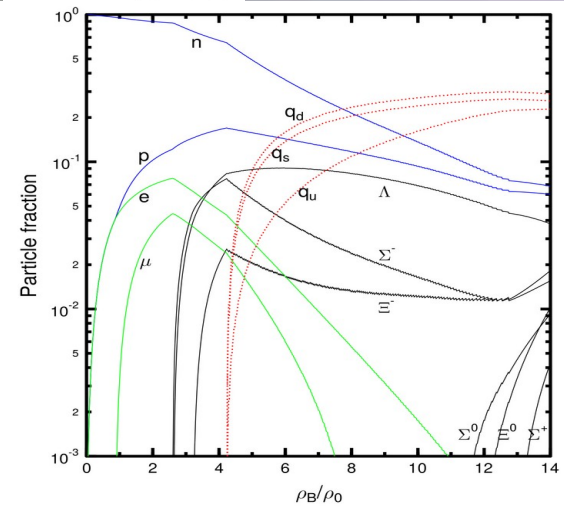$$\mu_i = B_i\,\mu_B + Q_i\,\mu_e$$

$$\begin{aligned} \mu_u &= \frac{1}{3}(\mu_B - 2\,\mu_e) \\ \mu_d = \mu_s &= \frac{1}{3}(\mu_B + \mu_e) \quad . \end{aligned}$$

The Gibbs Construction
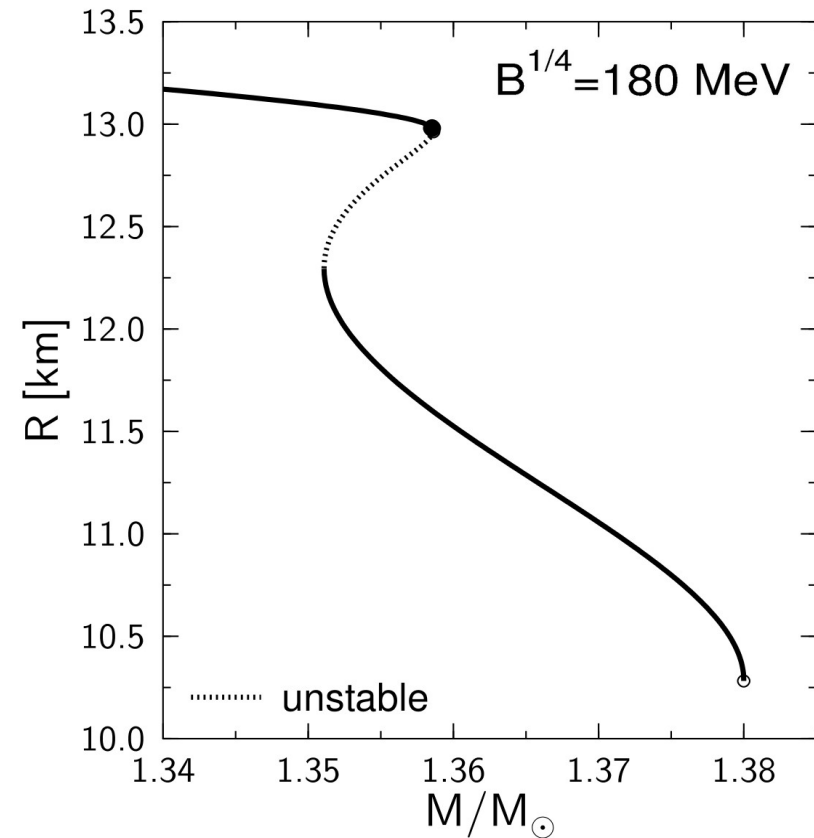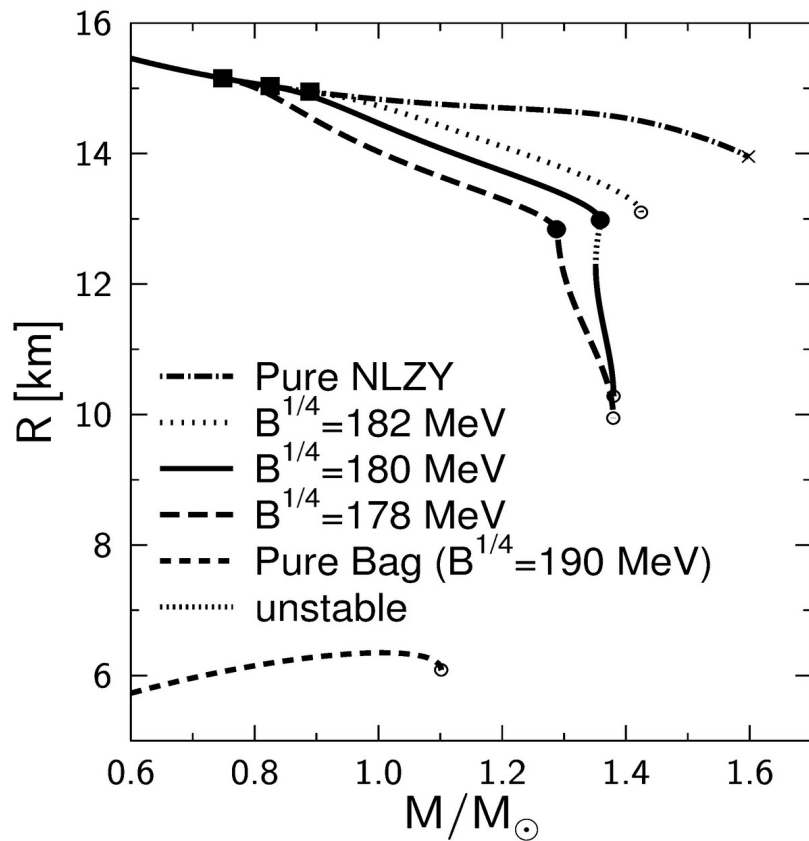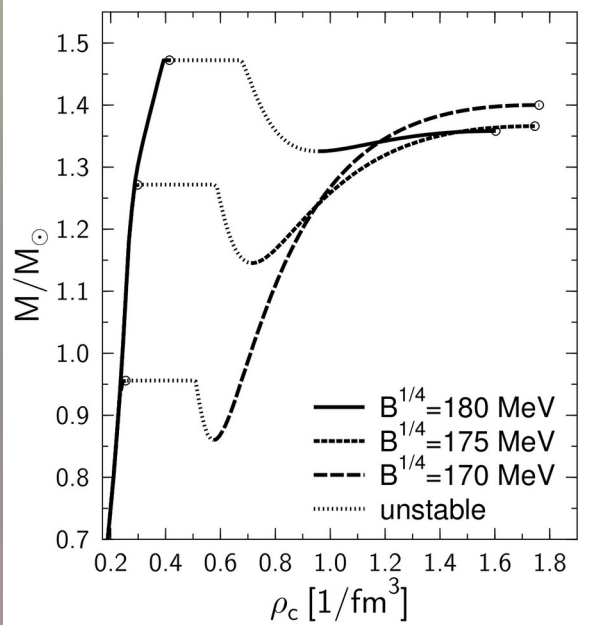
Hybrid Star Properties

Mass-Radius relations within a hybrid star model. The MIT-Bag model, for different values of the Bag parameter, was used for the quark phase, whereas for the hadronic phase the NLZY-model was used.

M. Hanauske, Dissertation, "Properties of Compact Stars within QCD-motivated Models"
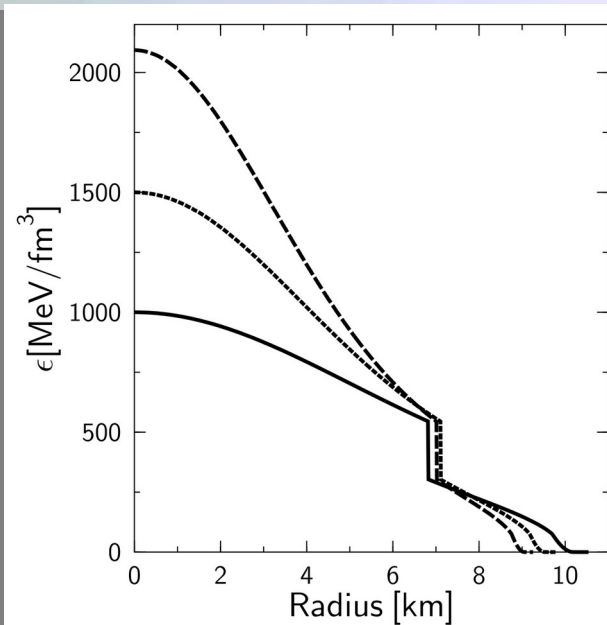
Hybrid Star Properties

In contrast to the Gibbs construction, the star's density profile within the Maxwell construction (see middle figure) will have a huge density jump at the phase transition boundary. Twin star properties can be found more easily when using a Maxwell construction (see left and right figure).
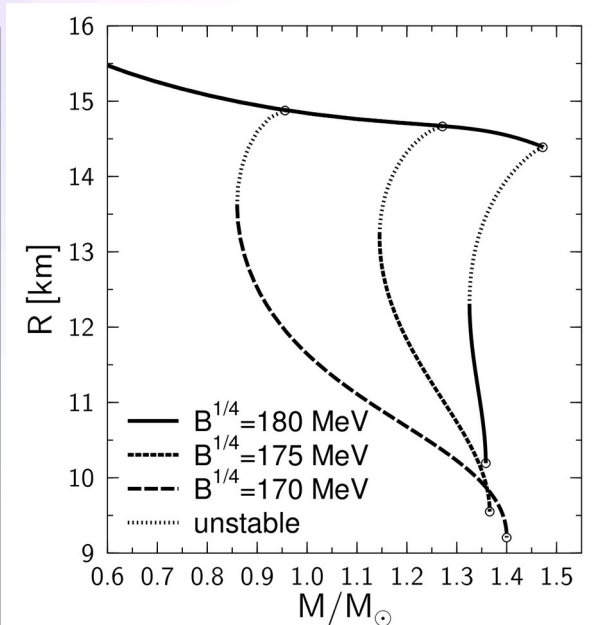
Mass-Density relation

Energy-density profiles

Radius-Mass relation

Matthias Hanauske: "How to detect the QGP with telescopes", GSI Annual Report 2003, p.96

Exotic Stars

But, unfortunately, twin stars can not be created solely by a Hadron-Quark phase transition. Extremely bound hyperon mater, or kaon condensation could also form a twin star behaviour.

J. Schaffner-Bielich, M. Hanauske, H. Stöcker, and W. Greiner, Phys. Rev. Lett. 89, 171101 (2002)
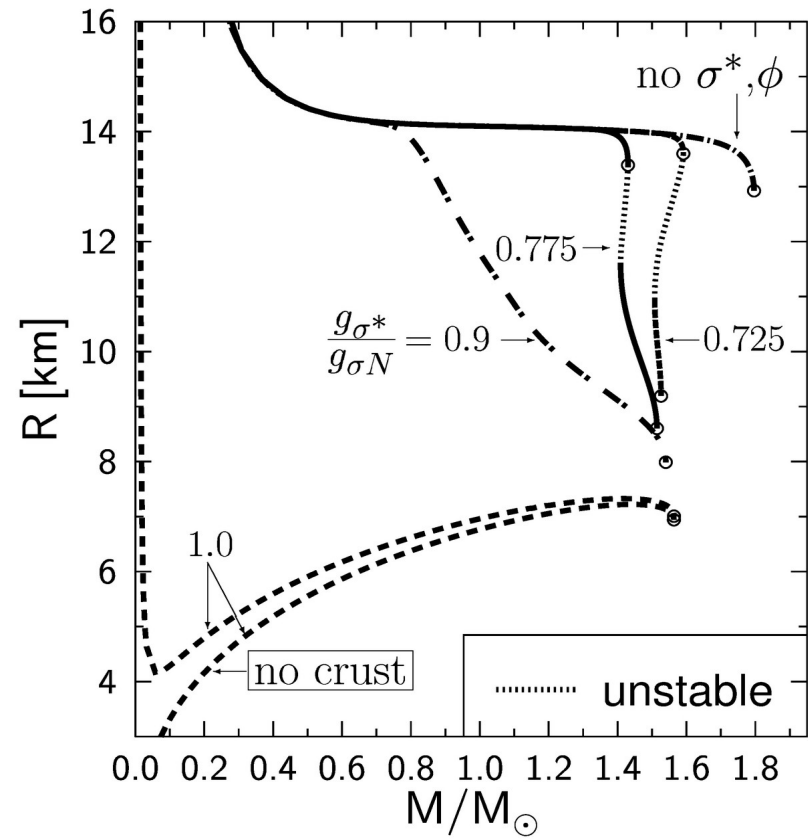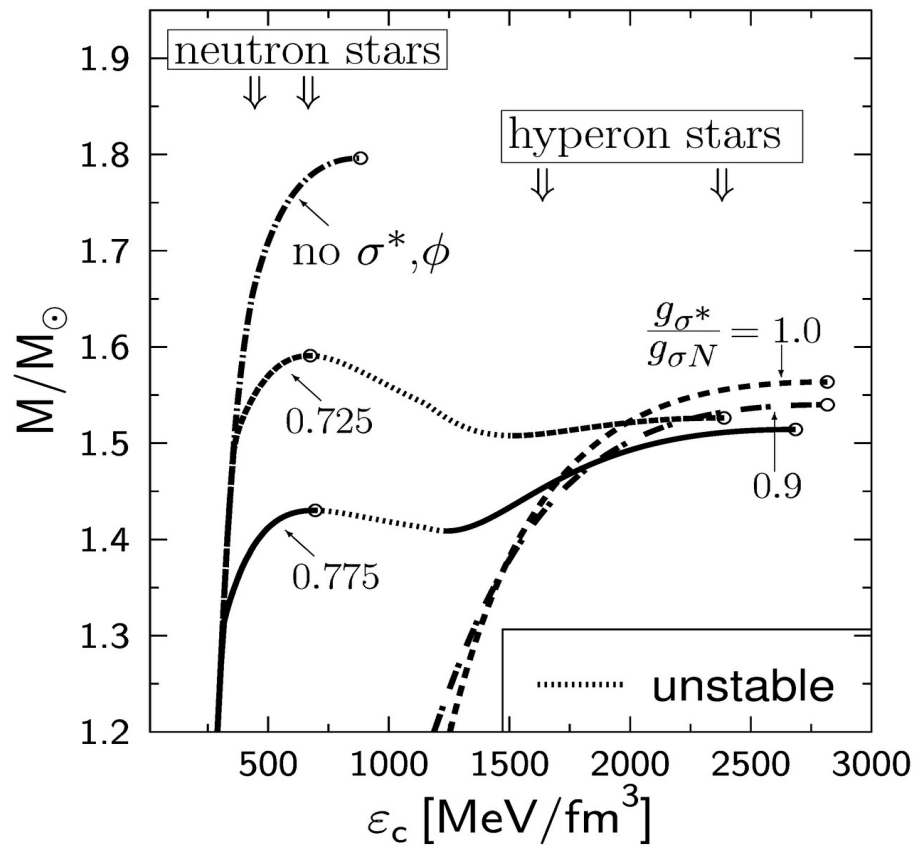
The Spin Up Effect

A rotating neutron star slowly loses its energy and angular momentum through electromagnetic and gravitational radiation with time. However, it conserves the total baryon number during this evolution. The Figures below show results of uniformly rotating compact stars including a Bose-Einstein condensates of antikaons. The Figure on the right shows the behavior of angular velocity with angular momentum. The mass shedding limit sequence is shown by a light solid line. The stable parts of the normal and supramassive sequences are displayed by dark solid lines and the unstable parts by dotted lines. Curve II indicates a collapse of a neutron star to an exotic star belonging to the third family of compact stars.

S. Banik, M. Hanauske, D. Bandyopadhyay, and W. Greiner, Phys. Rev. D 70, 123004 (2004)
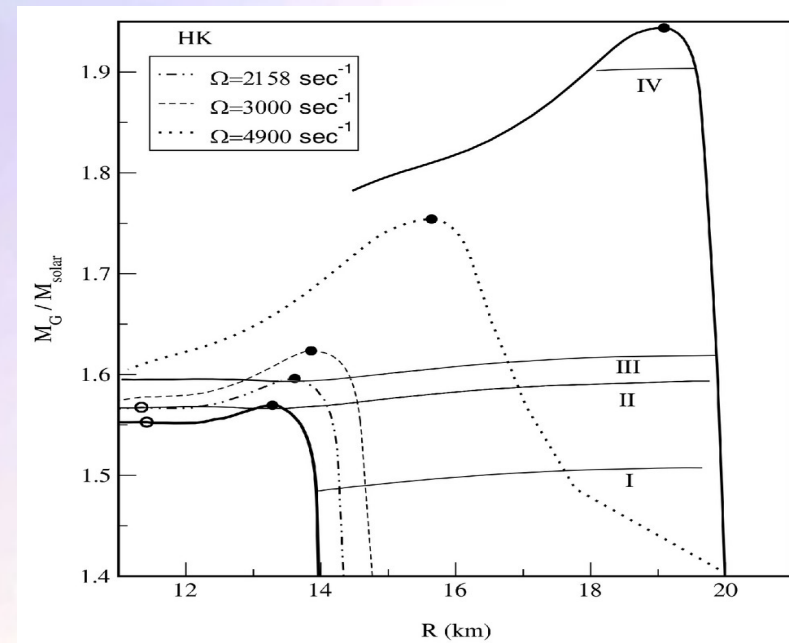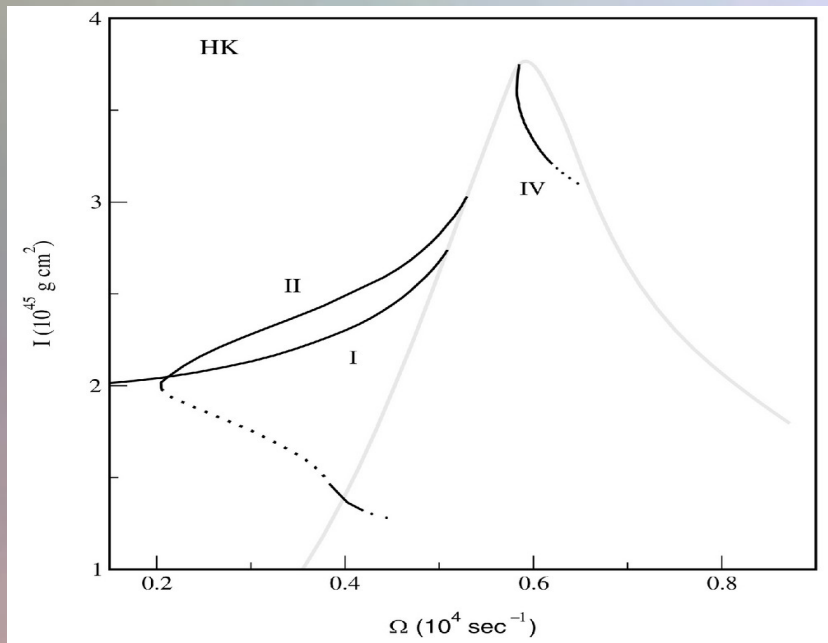
From ADM to BSSNOK

Unfortunately the ADM equations are only weakly hyperbolic (mixed derivatives in the three dimensional Ricci tensor) and therefore not "well posed". It can be shown that by using a conformal traceless transformation, the ADM equations can be written in a hyperbolic form. This reformulation of the ADM equations is known as the BSSNOK (Baumgarte, Shapiro, Shibata, Nakamuro, Oohara, Kojima) formulation of the Einstein equation. Most of the numerical codes use this (or the CCZ4) formulation.

The 3+1 Valencia Formulation of the Relativistic Hydrodynamic Equations

$$\nabla_\mu(\rho u^\mu) = 0,$$
$$\nabla_\nu T^{\mu\nu} = 0.$$

To guarantee that the numerical solution of the hydrodynamical equations (the conservation of rest mass and energy-momentum) converge to the right solution, they need to be reformulated into a conservative formulation. Most of the numerical "hydro codes" use here the 3+1 Valencia formulation.

Finite difference methods

Discretisation of a hyperbolic initial value boundary problem.
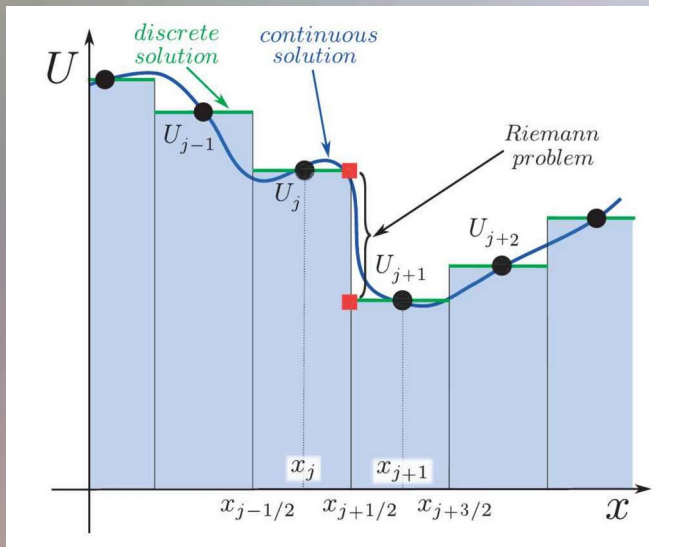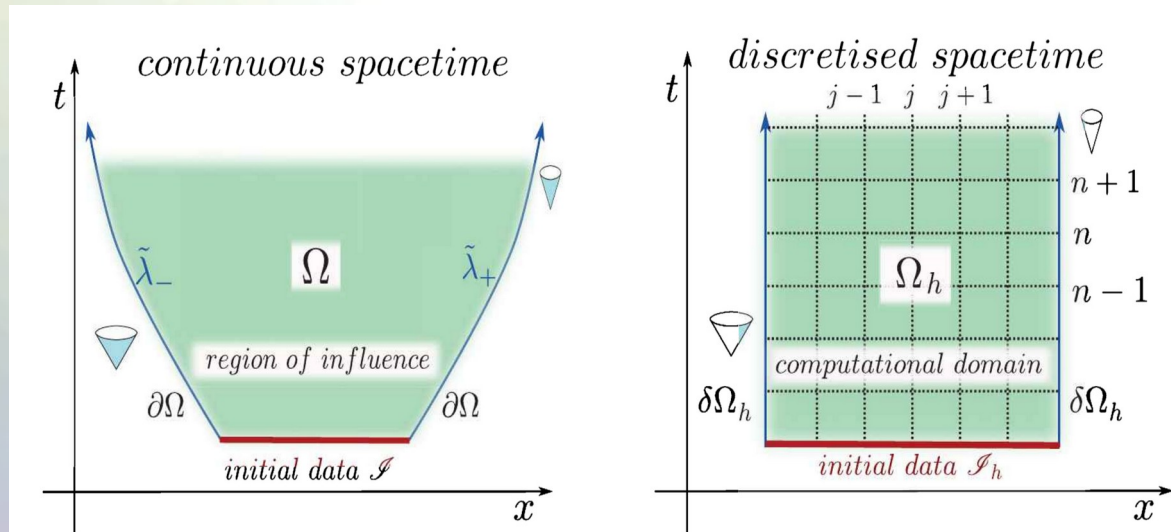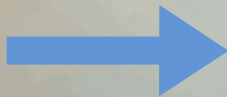
High resolution shock capturing methods (HRSC methods) are needed, when Riemann problems of discontinuous properties and shocks needs to be evolved accurately